İSTANBUL TECHNICAL UNIVERSITY ★ INSTITUTE OF SCIENCE AND TECHNOLOGY

SYNTHESIS OF ION-IMPRINTED POLYMERS AS RECOGNITION ELEMENTS IN CHEMICAL SENSORS

M.Sc. Thesis by
Salih SUBAŞI, B.Sc.

Department : Polymer Science and Technology
Programme: Polymer Science and Technology

Supervisor : Assoc.Prof. Orhan GÜNEY

JUNE 2008

İSTANBUL TEKNİK ÜNİVERSİTESİ ★ FEN BİLİMLERİ ENSTİTÜSÜ

KİMYASAL SENSÖRLERDE TANIMA ELEMANLARI OLARAK ION-IMPRINTED POLYMERLERİN KULLANILMASI

YÜKSEK LİSANS TEZİ

Salih SUBAŞI

Anabilim Dalı: Polimer Bilimi ve Teknolojisi
Programı: Polimer Bilimi ve Teknolojisi

Tez Danışmanı: Doç.Dr. Orhan GÜNEY

HAZİRAN 2008

İSTANBUL TECHNICAL UNIVERSITY ★ INSTITUTE OF SCIENCE AND TECHNOLOGY

SYNTHESIS OF ION-IMPRINTED POLYMERS AS RECOGNITION ELEMENTS IN CHEMICAL SENSORS

M.Sc. Thesis by
Salih SUBAŞI, B.Sc.
(515001124)

Date of submission : 5 May 2008

Date of defence examination: 11 May 2008

Supervisor (Chairman): Assoc. Prof. Dr. Orhan GÜNEY

Members of the Examining Committee Assoc. Prof. Dr. Filiz ŞENKAL (İTÜ)

Assoc. Prof. Dr. Cemal ÖZEROĞLU (İÜ)

JUNE 2008

İSTANBUL TEKNİK ÜNİVERSİTESİ ★ FEN BİLİMLERİ ENSTİTÜSÜ

KİMYASAL SENSÖRLERDE TANIMA ELEMANLARI OLARAK ION-IMPRINTED POLYMERLERİN KULLANILMASI

YÜKSEK LİSANS TEZİ

Salih SUBAŞI

Tezin Enstitüye Verildiği Tarih : 5 Mayıs 2008

Tez Danışmanı : **Doç.Dr. Orhan GÜNEY**

Diğer Jüri Üyeleri **Doç.Dr. Filiz ŞENKAL (İ.T.Ü)**

Doç.Dr. Cemal ÖZEROĞLU (İ.Ü.)

HAZİRAN 2008

ACKNOWLEDGEMENTS

I wish to express my appreciation to Assoc. Prof. Orhan GÜNEY, my supervisors, whose academic expertise, consistent direction and encouragement provided me with the inspiration to undertake and expand upon the research of this study.

I am also grateful to Zeki ARAR for trusting in me and giving me the opportunity to approach the thoughts that I only dreamt of.

I am deeply indebted to my family, who give their ever-present love and devotion, for all the guidance and support.

May, 2008 **Salih SUBAŞI**

TABLE OF CONTENTS

ACKNOWLEDGEMENTS iii
LIST OF ABBREVIATIONS vii
LIST OF SYMBOLS viii
LIST OF TABLES ix
LIST OF FIGURES x
SUMMARY xiii
ÖZET xv

1.INTRODUCTION 1

1.1. A History of Molecular Imprinting 1
1.2. Fundamental Aspects of Molecular Imprinting 2
1.3. Metal Ion-Mediated Polymers 3
1.3.1. Metal ion-mediated imprinting. 6
1.4. Synthesis and Synthesis Conditions of MIP Formation 7
1.4.1. Initiators 7
1.4.2. The effect of temperature and other polymerization conditions 8
1.4.3. Cross-linkers 8
1.4.4. Porogen effects 9
1.5. Recognition and Binding 9
1.5.1. Template studies 9
1.5.2. Solvent effects in binding 10
1.5.3. Selection approaches to MIP optimization 11
1.5.4. Chemical and physical post-treatment of MIPs 11
1.6. Thermodynamics, Physical Characterization and Modeling 12
1.6.1. Thermodynamic aspects and modeling of the pre-polymerization complex 12
1.6.2. Spectroscopic studies of the pre-polymerization complex 13
1.6.3. Modeling polymer formation in the presence of templates 14
1.6.4. Characterizing the binding sites and their distribution 15
1.6.5. Physical methods of characterizing the rebinding event 15
1.7. Parameters Involved in Molecular Recognition Events 16
1.7.1. Molecular interactions involved in non-covalent imprinting 17
1.8.Sensors Iinvolving Molecularly Imprinted Polymers 18
1.8.1. Fluorescence-based sensing devices 19
1.8.2. Optical sensors 22
1.9. Fluorescence Spectroscopy 23
1.9.1. Jablonski diagram 23
1.9.1.a. Fluorescence 24
1.9.1.b. Intersystem crossing 25
1.9.2. Characteristics of fluorescence emission 25
1.9.2.a. Stokes Shift 25

1.9.2.b. Kasha's rule 25
1.9.2.c. Mirror image rule 26
1.9.3. Fluorescence quenching 26
1.9.3.a. Coalitional quenching 27
1.9.3.b. Mechanisms of quenching 27
1.9.3.c. Stern-Volmer plot 27
1.9.3.d. Static quenching 27
1.9.3.e. Both static and dynamic quenching can have a linear Stern-Volmer plot 28
1.9.3.e. Both static and dynamic quenching can have a linear Stern-Volmer plot 29

2.EXPERIMENTAL 29
2.1 Materials 29
2.2. Structure of Fluorescent Monomers Used in Synthesis of Polymeric Materials 29
2.3. Synthesis of Lead-ion Imprinted Sensor Containing VCz 29
2.3.1. Removal of the lead-ion from the synthesized polymers 30
2.4. Synthesis of Iron-Ion Imprinted Sensor with VCz 30
2.4.1. Removal of the iron-ion from the synthesized polymers 30
2.4.2. Synthesis of the control polymer particles 31
2.5. Synthesis of Copper-Ion Imprinted Sensor with VCz 31
2.5.1. Removal of the copper-ion from the synthesized polymers 31
2.6. Synthesis of Zinc-ion Imprinted and Nonimprinted Polymers with BCM 31
2.7. Synthesis of Copper-Ion Iimprinted and Nonimprinted Polymers with BCM 32
2.8. FTIR-ATR(Attenuated Total Reflectance-Infrared) Spectroscopy 32
2.9. Fluorescence Measurements 32

3.RESULT AND DISCUSSION 34
3.1.Interaction of VCz with Metal Ion 34
3.1.1. FTIR-ATR spectra of Pb-imp and nonimp polymers 36
3.1.2. Pb^{2+} binding capability of Pb-imp and nonimp materials 37
3.1.3. Comparison of Fe^{2+} affinities of Fe-imp and nonimp polymers 42
3.1.4. Affinities of Cu-imp and nonimp materials to Cu^{2+} 44
3.2. Photophysical Properties of BCM 47
3.2.1. Titration of BCM with metal ıon 48
3.2.2. FTIR-ATR spectra of Zn-imp and nonimp polymers 53
3.2.3. Fluorescence spectra of Zn-imp and nonimp polymers containing BCM against to pH 54
3.2.4. Response of cylindrical Zn-imp and nonimp polymers containing BMC to Hg^{2+} 57
3.2.5. Affinities of semi-cylindrical Cu-imp and nonimp polymers containing BCM to Cu^{2+} 60

5. CONCLUSIONS **62**

REFERENCES **64**

BIOGRAPHY **78**

ABBREVIATIONS

MIPs : Molecularly Imprinted Polymer
IIPs : Ion-imprinted polymers
MAA : Methacrylic Acid
MMA : Methyl methacrylate
EGDM : Ethyleneglycol dimethacrylate
AIBN : 2,2'-azobisisobutyronitrile
VCz : 9-vinylcarbazole
VIm : Vinyl imidazole
ABDV : 2,2'-azobis(2,4-dimethylvaleronitrile)
ABCHC : 2,2'-azobis(cyclohexylcarbonitrile)
SERS : Surface-enhanced Raman scattering
TEMED : *N,N,N',N'*-tetramethylenediamine
FLD : Fluorescence Detector
IMP : Imprinted
IR : Infrared
PbMAA2 : Lead methacrylate
FLU : fluorescence
AA : Acrylamide
MeCN : Acetonitrile
HX : acid
X : wavelength
L : Ligand
R : Relaxation Rate
BCM : Benzofuran chalcone methacrylamide
FTIR-ATR : Attenuated Total Reflectance-Infrared

LIST OF SYMBOLS

F_0	**:** Observed fluorescence in the absence of quencher
F	**:** Observed fluorescence in the presence of quencher
k_q	**:** Bimolecular quenching constant
K	**:** Stern-Volmer quenching constant
[Q]	**:** Quencher concentration
Mg	**:** milligram
mL	**:** milliliter
mmol	**:** millimole
mol	**:** mole
s	**:** seconds

LIST OF TABLES

PageNo

Table 1.1 : Parameters contributing to molecular recognition…….. 16
Table 1.2 : Hydrogen bonding donor and acceptor groups…….. 17
Table 1.3 : Types and estimated bond energies of non-covalent interactions… 18

LIST OF FIGURES **Page No:**

Figure 1.1 : Schematic representation of the molecular imprinting……. 3
Figure 1.2 : Jablonski Energy Diagram……..... 24
Figure 1.3: The chemical structure of VCz and BCM……. 29
Figure 3.1: Excitation spectra of $4x10^{-5}$ M VCz in acetonitrile in the presence of different concentration of Cu^{2+}.($\lambda_{em} = 367$)……..... 34
Figure 3.2: Emission spectra of $4x10^{-5}$ M VCz in acetonitrile depending on Cu^{2+} concentration ($\lambda_{ex} = 332$)…….. 35
Figure 3.3: Stern-Volmer plot of emission of $4x10^{-5}$ M VCz in acetonitrile quenched by Cu^{2+} ion. ($\lambda_{ex} = 332$)……... 36
Figure 3.4 : FTIR-ATR spectra of Pb-imp and nonimp polymers…….. 37
Figure 3.5: Effects of Pb^{2+} concentrations on the fluorescence spectra of Pb-imp sensor containing PVCz. (λ_{ex} = 332 nm)…… 38
Figure 3.6: Emission spectra of nonimp polymer containing PVCz depending on Pb^{2+} concentrations(λ_{ex} = 332 nm)……. 38
Figure 3.7 : Pb^{2+} dependence of emission intensity of Pb-imp and nonimp polymers Containing PVCz. (λ_{ex} = 332 nm)…… 39
Figure 3.8 : Fluorescence emission spectra of Pb-imp sensor in the presence of different concentration of Pb^{2+} ion in aqueous solution containing 0.1 M $NaNO_3$…….. 40
Figure 3.9 : Fluorescence spectra of nonimp polymer in the presence of different concentration of Pb^{2+} ion in aqueous solution containing.. 0.1 M $NaNO_3$ 40
Figure 3.10 : Dependence of emission intensity of Pb-imp and nonimp polymers containing PVCz to the Pb^{2+} concentration in 0.1 M $NaNO_3$ ($\lambda_{ex} = 332$ nm)…… 41
Figure 3.11: Plot of I / I_0 for Pb-imp and nonimp polymers as a function of time obtained in the presence of $5x10^{-4}$ M Hg^{2+} in aqueous solution.($\lambda_{ex} = 332$ nm)……. 42
Figure 3.12: Emission spectra of Fe-imp sensor containing PVCz upon Fe^{2+} concentrations in aqueous solution. ($\lambda_{ex} = 332$ nm.)…… 43
Figure 3.13: Dependence of emission spectra of nonimp polymer containing PVCz in the presence of Fe^{2+} concentrations in aqueous solution. ($\lambda_{ex} = 332$ nm.)…….. 43
Figure 3.14: Changing of emission intensity of Fe-imp and nonimp polymers containing PVCz depending on Fe^{2+} concentrations. Emission spectra were obtained after waited 30 minute in the presence of Fe^{2+} metal ions. ($\lambda_{ex} = 332$ nm)……..... 44
Figure 3.15: Fluorescence emission spectra of Cu-imp sensor containing PVCz depending on Cu^{2+} concentrations. ($\lambda_{ex} = 332$ nm)…… 45

Figure 3.16: Emission spectra of nonimp polymer in the presence of Cu^{2+} concentrations. Emission spectra were obtained after waited 30 minute in the presence of metal ions…… 46
Figure 3.17: Changing of I / I_0 values at 367 nm of Cu-imp and nonimp polymers versus Cu^{2+} concentrations. ($\lambda_{ex} = 332$ nm)…… 46
Figure 3.18: Excitation and emission spectra of BCM in DMSO depending concentration . ($\lambda_{ex} = 410$ nm and $\lambda_{em} = 510$ nm)…… 47
Figure 3.19: Emission intensities of BCM in DMSO depending on concentration. $\lambda_{ex} = 410$ nm.…… 48
Figure 3.20 : Fluorescence spectra of $2x10^{-5}$ M BCM in DMSO depending on Cu^{2+}. ……. 49
Figure 3.21: Cu^{2+} dependence of emission intensity at 510 nm of $2x10^{-5}$ M BCM in DMSO. ($\lambda_{ex} = 410$ nm.…… 49
Figure 3.22: Emission spectra of $2x10^{-5}$ M BCM in ethanol in the presence of Hg^{2+}. ($\lambda_{ex} = 410$ nm)…… 50
Figure 3.23: Emission spectra of $2x10^{-4}$ M BCM in ethanol depending on Titration with Hg^{2+}.($\lambda_{ex} = 410$ nm)…… 50
Figure 3.24: Dependence of emission intensities of BCM at different concentrations to Hg^{2+}.($\lambda_{ex} = 410$ nm)…… 51
Figure 3.25: Excitation and Emission spectra of $2x10^{-5}$ M BCM in 2-Methoxy ethanol depending on titration with Hg^{2+} ($\lambda_{ex} = 410$ nm and $\lambda_{em} = 500$ nm) …… 51
Figure 3.26 : Excitation and Emission spectra of $2x10^{-5}$ M BCM in acetonitrile depending on titration with Hg^{2+}. ($\lambda_{ex} = 410$ nm and $\lambda_{em} = 500$ nm)…….. 52
Figure 3.27: Hg^{2+} dependence of emission intensity of $2x10^{-5}$ M BCM in different solvents……... 53
Figure 3.28: FTIR-ATR spectra of Zn-imp and nonimp polymers containing BMC…….. 53
Figure 3.29: Fluorescence response of Zn-imp plane sensor containing BCM against to pH in base solution. ($\lambda_{ex} = 410$ nm)…… 54
Figure 3.30: pH dependence of fluorescence spectra of nonimp polymer containing BCM in base solution. ($\lambda_{ex} = 410$ nm)……..... 55
Figure 3.31: Fluorescence emission intensities of Zn-imp and nonimp polymers containing BCM against to pH. ($\lambda_{ex} = 410$ nm)…… 55
Figure 3.32: Fluorescence response of Zn-imp plate sensor containing BCM against to pH in acid solution. ($\lambda_{ex} = 410$ nm)……. 56
Figure 3.33: pH dependence of fluorescence spectra of nonimp polymer containing BCM in acid solution. ($\lambda_{ex} = 410$ nm)……. .. 57
Figure 3.34: Fluorescence response of Zn-imp and nonimp polymers against to pH…… 57

Figure 3.35: Fluorescence Emission spectra of cylindrical Zn-imp sensor Containing BCM depending on Hg^{2+} concentrations. ($\lambda_{ex} = 410$ nm)……. 58

Figure 3.36 : Emission spectra of cylindrical nonimp polymer containing BCM upon titration with Hg^{2+} ion concentration in aqueous solution ($\lambda_{ex} = 410$ nm)……. 59

Figure 3.37: Emission intensities of cylindrical Zn-imp and nonimp Polymers containing BCM in the presence of Hg^{2+} concentrations.($\lambda_{ex} = 410$ nm)…….… 59

Figure 3.38: Fluorescence emission spectra of semi-cylindrical Cu-imp Sensor containing BCM as a function of Cu^{2+} concentrations in DMSO.($\lambda_{ex} = 410$ nm)…….. 60

Figure 3.39: Emission spectra of semi-cylindrical nonimp polymer containing BCM depending on Cu^{2+} concentrations in DMSO. ($\lambda_{ex} = 410$ nm)…… 61

Figure 3.40: Cu^{2+} dependence of emission intensities of semi-cylindrical Cu-imp and nonimp polymers containing BCM in DMSO. ($\lambda_{ex} = 410$ nm)…… 61

SYNTHESIS OF ION-IMPRINTED POLYMERS AS RECOGNITION ELEMENTS IN CHEMICAL SENSORS

SUMMARY

In first part of the study, metal ion binding property of 9-vinyl carbazole (VCz) monomer in different solvents was investigated by fluorescence spectroscopy. Imprinted polymeric materials containing VCz as a fluoroprobe molecule were synthesized in the presence of template forming metal ions. Randomly synthesized polymers which are called nonimprinted materials were obtained in the absence of metal ions. Characterization and determination of identical structures of imprint and nonimprint polymeric materials after removal of metal ions by washing procedure were elucidated by FTIR-ATR spectroscopic measurements. Metal ion binding properties of imprinted and nonimprinted materials, which were synthesized in different geometrical shapes, were explored by analyzing fluorescence excitation and emission spectra depending on the metal ion concentration and different electrolyte conditions.

In the second part of the study, photophysical and metal ion binding properties of newly synthesized Benzofuran Chalcone Methacrylamide (BCM) monomer were explored. Fluorescence titration measurements were conducted to elucidate the metal ion binding affinity of BCM in different solvents which have different dipol moments and dielectric constants. The selectivity of BCM towards biologically important metal cations was analyzed using Stern-Volmer equations. Metal-ion templated polymers as imprinted sensors and random polymers as nonimprinted materials containing BCM as a fluorescent probe were synthesized in different geometric shapes. FTIR-ATR spectroscopic measurements were conducted to characterize and determine the identical structures of imprint and nonimprint polymers washed consecutively with acid aqueous and organic solutions for removing metal ions and unreacted monomers.

Then the metal ion adsorption experiments were carried out to elucidate the imprinting properties of polymers containing BCM by comparing the fluorescence quenching efficiency of imprinted and nonimprinted materials used in chemical sensing measurements against target metal ions.

All imprinted and non-imprinted polymeric materials containing VCz and BCM molecules as fluorescent probe were synthesized in form of plate, semi-cylindrical and cylindrical shapes and designed to be used as recognition elements in chemical sensors.

KİMYASAL SENSÖRLERDE TANIMA ELEMANLARI OLARAK ION-IMPRINTED POLYMERLERİN SENTEZİ

ÖZET

Çalışmanın ilk kısmında, 9-vinil karbazol (VCz) monomerinin farklı çözücüler içindeki metal bağlama özelliği floresans spektroskopisi ile incelendi. Floresans kılavuz olarak VCz içeren imprint polimerik malzemeler şablon oluşturucu metal iyon varlığında sentezlendi. Nonimprint malzemeler olarak adlandırılan rastgele sentezlenmiş polimerler, ortamda metal iyonları olmadan elde edildi. Yıkama prosedürü ile metal iyonlarının uzaklaştırılmasından sonra imprint ve nonimprint malzemelerin benzer yapılarının belirlenmesi ve karakterize edilmesi FTIR-ATR spektroskopik ölçümlerle gerçekleştirildi. Farklı geometrik şekillerde sentezlenen imprint ve nonimprint malzemelerin metal bağlama özellikleri, farklı elektrolit koşullarında ve metal iyonu konsantrasyonuna bağlı olarak floresans eksitasyon ve emisyon spektrumaları analiz edilerek araştırıldı.

Çalışmanın ikinci kısmında, yeni sentezlenen benzofuran kalgon metakrilamid (BCM) monomerinin fotofiziksel ve metal iyon bağlama özellikleri araştırıldı. Farklı dipol momente ve dielektrik sabitine sahip çözücüler içinde BCM nin metal bağlama özellikleri floresans titrasyon ölçümleri gerçekleştirilerek açıklığa kavuşturuldu. Biyolojik öneme sahip metal katyonlarına karşı BCM nin seçiciği Stern-Volmer denklemleri kullanılarak analiz edildi. Floresant kılavuz olarak BCM içeren, imprint sensör olarak metal iyonla şablonlanmış polimerler ve nonimprint malzeme olarak rastgele polimerler farklı geometrilerde sentezlendi. Metal iyonlarını ve reaksiyona girmemiş monomerleri uzaklaştırmak için organik ve sulu asit çözeltileri içinde sırasıyla yıkanan imprint ve nonimprint polimerlerin özdeş yapılarını belirlemek ve karakterize etmek için FTIR-ATR spektroskopik ölçümler gerçekleştirildi. Daha sonra BCM içeren polimerlerin imprint özelliklerini aydınlatmak için hedef metal iyona karşı kimyasal algılama ölçümlerinde kullanılan imprint ve nonimprint malzemelerin floresans sönümlendirme etkinlikleri karşılaştırılarak metal adsorpsiyon ölçümleri gerçekleştirildi.

Floresant klavuz olarak VCz ve BCM içeren imprint ve nonimprint bütün polimerik malzemeler plaka, yarı silindirik ve silindirik formda sentezlendi ve kimyasal sensörlerde tanıma elemanı olarak kullanılmak üzere dizayn edildi.

1. INTRODUCTION

1.1 A History of Molecular Imprinting

The dramatic increase in the volume of literature describing the design, development and application of molecularly imprinted polymers (MIPs) over recent years reflects the maturation of this field of study and the broad interest it has attracted from the scientific community in general. The concept of a molecularly imprinted polymer has evolved to include a vast array of organic polymers and polymer formats. The number of reviews on the topic of molecular imprinting has increased along with the rapidly expanding primary literature dealing with the area. Most of the initial efforts to review the field aimed to encompass essentially all work which was known at that point in time.[1] Contributions related to molecular imprinting have also appeared in many multi-authored monographs and general scientific reference works.[2] More recently, a combination of the sheer volume of the literature related to the field together with the breadth of development in some application areas has resulted in many more specialized reviews and contributions to monographs focussing upon specific aspects of molecular imprinting science and technology. Furthermore, reviews covering aspects of molecular imprinting are now often found presented in conjunction with cognate techniques.

More recently, a series of books on the topic have been forthcoming, which in many cases has provided the scientific public with consolidated presentations of various aspects of the design, preparation, characterization and application of molecularly imprinted polymers. Currently two fundamental approaches to molecular imprinting may be distinguished. One of these is covalent or preorganized approach mainly developed by Wulff and Sarhan, where the template–monomer construct in solution prior to polymerization is maintained by reversible covalent bonds and the recognition of the template is dependent on the formation and cleavage of these bonds.

The other major type is the non-covalent imprinting or self-assembly approach, advocated mainly by Mosbach and co-workers, where the pre-arrangement between the template and monomer(s) is formed by non-covalent interactions and subsequent recognition is also dependent on these interactions. In parallel with these strategies, another method—semi-covalent approach termed as sacrificial spacer methodology has been introduced which takes the advantage of a combination of the above approaches, with strong covalent bonds being used in the imprinting step, and non-covalent interactions used in the recognition process after cleavage of the template from the polymer.

1.2. Fundemantal Aspects of Molecular Imprinting

Molecular imprinting is an example of molecular recognition by self-assembly, rather than by design and may use common vinyl monomers to achieve a high degree of selectivity in what can be a very robust material. [3] Molecular recognition is a phenomenon that can be envisaged as the preferential binding of a molecule to a "receptor" with high selectivity over closely related structural analogues. This concept has been translated elegantly into the technology of molecular imprinting, which allows specific recognition sites to be formed in synthetic polymers through the use of various templates. [4, 5] The construction of ligand selective recognition sites in synthetic polymers where a template (atom, ion, molecule, complex or a molecular, ionic or macromolecular assembly, including micro-organisms) is employed in order to facilitate recognition site formation during the covalent assembly of the bulk phase by a polymerization or polycondensation process, with subsequent removal of some or all of the template being necessary for recognition to occur in the spaces vacated by the templating species[6]. Schematically this can be represented by Figure 1.1.

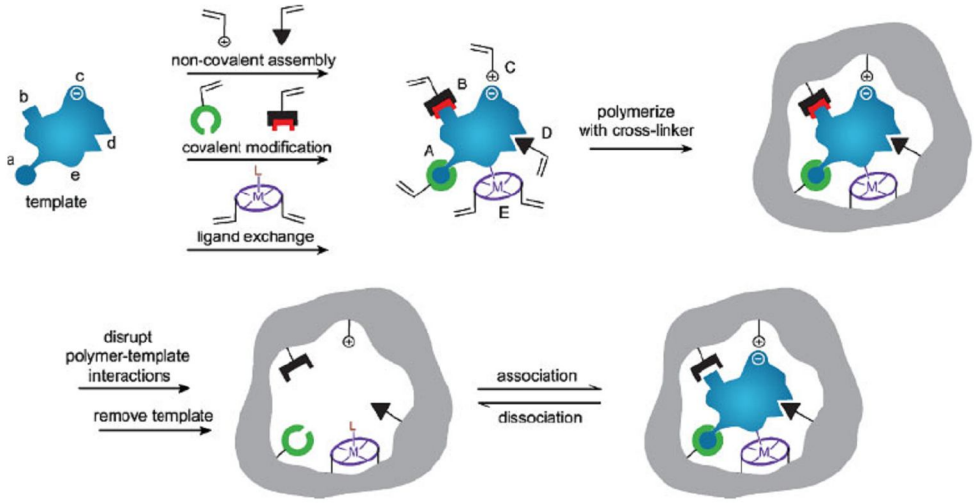

Figure 1.1 Schematic representation of the molecular imprinting process

The formation of reversible interactions between the template and polymerizable functionality may involve one or more of the following interactions: (A) reversible covalent bond(s), (B) covalently attached polymerizable binding groups that are activated for non-covalent interaction by template cleavage, (C) electrostatic interactions, (D) hydrophobic or van der Waals interactions or (E) co-ordination with a metal centre; each formed with complementary functional groups or structural elements of the template, (a-e) respectively]. A subsequent polymerization in the presence of crosslinker(s), a cross-linking reaction or other process, results in the formation of an insoluble matrix (which itself can contribute to recognition through steric, van der Waals and even electrostatic interactions) in which the template sites reside. Template is then removed from the polymer through disruption of polymer—template interactions, and extraction from the matrix. The template, or analogues thereof, may then be selectively rebound by the polymer in the sites vacated by template, the 'imprints'. While the representation here is specific to vinyl polymerization, the same basic scheme can equally be applied to sol-gel, polycondensation etc.

1.3 Metal ion-Imprinted Polymers

Ion-imprinted polymers (IIPs) are similar to MIPs, but they recognize metal ions after imprinting, while retaining all the virtues of MIPs. There have been numerous reports describing strategies for the imprinting of metal ions.[7]

One approach involves the cross-linking of linear polymers containing groups capable of metal binding. Pioneering work was carried out by Nishide et al. who cross-linked poly(4-vinylpyridine) in the presence of transition metal ions with dibromo-compounds. Similarly a preformed transition metal complex with partially quaternized poly(4-vinylpyridine)or poly(vinylphosphonic acid-co-acrylic acid) was cross-linked with N,N^0 -methylene-bisacrylamide. Other linear polymer systems which have been cross-linked by a post-polymerization method in the presence of a metal are chitosan, [8] polyethyleneimine [9, 10] andpolystyrene-co-acrylamide. [11] Kabanov et al. cross-linked a copolymer of diethylvinylphosphonate and acrylic acid with *N*-methylene diacrylamide in the presence of metal ions. Prasada Rao et al. has reviewed recently on the topic entitled "Tailored ion-imprinted polymer materials for solid phase extraction of inorganics". Of the various factors that have been identified for the formation and the recognition properties of binding sites, multiple site interactions with the functional monomers are likely to yield binding sites of higher specificity and affinity. The binding strength of polymer as well as the fidelity in the recognition depends on the number and type of interaction sites, the template shape and the monomer-template rigidity. Thus, better fit between the site and the template lead to less entropy loss due to the conformational changes in the site as well as in the template upon rebinding. This will increase the affinity and selectivity in the recognition. These metal ion templates are embedded rigidly in polymeric matrices which can result in IIPs with different configurations, viz. particles, beads or microspheres depending on the polymerization method. Applications of such IIPs include solid phase extraction, metal ion sensors (selectrodes and optrodes) and membranes. The number of papers, which feature the term ion-imprinted polymer, though initiated in 1976, has increased dramatically over the last few years. This review attempts to give an accessible summary of the field, where the trends can be identified in synthetic approaches and characterization of IIPs and opens up possibilities for new preconcentrative separations, sensing and possibly even membrane-based technologies.

Metal-imprinted hydrogels have been reported [12] in which a linear polymer was first incubated with the metal ion, with subsequent formation of interpenetrating networks. The imprinting of alginate gels with copper ions has been reported. [13]

Metal imprinted films have been constructed by casting linear co-polymers in the presence of a transition metal ion.[14] The physical immobilization of a chelator (dithizone), in complexation with different transition metals in various linear polymers, has also been described.[15] Another approach to the synthesis of metal-MIPs is the initial formation of a complex between the metal ion and polymerizable ligand (functional monomer) which is then polymerized with cross-linker. Polymerizable ligands that have been used include: 1-vinylimidazole, 4′-methyl-4-vinylbipyridine, MAA, vinylbenzoic acid,[16] 2-acetyl-5-(p-vinylbenzyloxy)phenol, vinyl dithiophosphinates, chloroacrylic acid, vinylpyri-dine,[17,18] polymerizable derivatives of diethylene triamine pentaacetic acid [19] and triethylenetetramine,[20] N-(4-vinylbenzyl)-1,4,7-triazacyclononane, Ni(II)-selec-tive ligands, a polymerizable ionophore, 9-vinylcarbazole (fluorescent monomer),[21] methyl-3,5-divinylbenzoate (luminescent monomer) [22] and methacryloylamidohisti-dine.[23] Palladium and uranyl ions have been imprinted using vinylpyridine as functional monomer with a non-polymerizable ligand.[24–25] Metal ions have also been imprinted using sandwich complexes co-polymerized with DVB;[26] the imprinting of an entire organometallic complex, without polymerizable ligands, has also been carried out[27] and MIPs for ferrocyanide ion have also been reported.[28] Enzymatic free radical coupling was investigated as a potential method to construct ion-selective MIPs.[29] The synthesis of ion-imprinted polymers inside solid supports, i.e. Amberlite XAD [30] and silica gel,[31] has been reported, and the use of a reversible cross-linker on Ca^{2+} absorption has been investigated. Imprinted ion exchange resins for UO_2^{2+} and Th^{4+} have been reported.

A number of approaches to the imprinting of metal ions on surfaces have been described. One such method involves polymerization at a water–oil interface and was first reported by Kido et al.[32] Functional surfactants were used to complex metal ions dissolved in the aqueous phase, while stabilizing a monomer suspension. The surfactant–template complex was subsequently immobilized through polymerization of the oil phase resulting in a surface-confined imprint site.[33] The preparation of similar surface-imprints for metal ions in a seeded emulsion polymerization was described by Takagi and coworkers. Other reports also describe metal-ion imprinting in organic polymers.[34]

The possibility of using waste biomass, for example the mycelium of Penicil-lium chysogenum, as a supportive matrix which was surface coated with chitosan in the presence of Ni^{2+} has recently been investigated.[35] There are also a number of reports of the imprinting of metal ions in sol-gel [36,37] matrices.

1.3.1. Metal ion-mediated imprinting.

Metal ions have the ability to bind to a wide range of functional groups through the donation of electrons from the heteroatoms of ligands to the unfilled orbitals of the outer coordination sphere of the metal. The strength of interaction can vary enormously from weak, readily exchangeable bonds to strong bonds which behave like covalent links, depending on the metal, its oxidation state and ligand characteristics. Consequently metal coordination has been employed as an alternative means of association between template and functional monomer in the construction of imprinted polymers.[38] The complex used for imprinting generally consists of polymerizable ligand(s) to complex the metal ion (generally a transition metal ion) which in turn coordinates to the template.

This approach was first reported by Fujii et al. in the imprinting of amino acids. The group of Arnold investigated different metals and polymerizable ligands for the imprinting of templates including bisimidazoles in organic matrixes and on solid supports. Copper(II) was employed as a coordination metal for the synthesis of carbohydrate-selective polymers.[39] Other molecules imprinted via this approach include a chiral bi-2-naphthol,[40] 1,10-phena-throline,[41] gluconamide, histamine,[43] amino acids, peptides[43] and proteins. The use of dendritic structures as an aid in the production of chiral imprints at Pt has also been reported.[44] Polymerizable ligands based on porphyrin have been described for the imprinting of N-heterocyclic templates in sol-gel materials and in polymeric matrixes.[45] A recognition site for dioxygen was created using metal ion-mediated imprinting.[46,47] Recently it was shown that imprinted polymers prepared for cholesterol using Cu^{2+} acrylate, in place of acrylic acid, resulted in MIPs with higher capacities,[48] and a ferric acrylate-containing MIP for cholesterol has also been reported.[49] The importance of the presence of the metal ion in the rebinding step has been shown.[50,51] A number of catalytic imprinted polymers have been fabricated using ion-mediated imprinting (for references see Catalysis part).

The use of Eu^{3+} as coordination metal results in materials which can be employed in luminescent sensors.[52–53]

1.4. Synthesis Conditions of MIP Formation

1.4.1 Initiators

Thermal decomposition of azo-initiators is the most commonly used source of free radicals in the formation of both DVB- and (meth)acrylate-based MIPs, azo-bis-isobutyronitrile (AIBN) being the standard. The photochemical decomposition of this compound allows MIPs to be prepared at low temperature,[54] with a resultant increase in separation efficiency of the polymers. The initiator 2,2'-azobis(2,4-dimethylvaleronitrile) (ABDV) has athermal decomposition temperature lower than that of AIBN and allows thermal polymerization to be initiated at 40°C. The initiator 2,2'-azobis(cyclohexylcarbonitrile) (ABCHC) has solubility superior to that of AIBN at low temperatures which may be an advantage in photochemical initiation.[55,56] Functionalized azo-initiators, such as 4,4'-azobis(4-cyanopentanoic acid), have been attached to surfaces for grafting of MIPs to capillaries [57] or silica beads.[58] Other thermal initiators include organic peroxides such as benzoyl peroxide , and lauroyl peroxide or water-soluble inorganic initiators such as ammonium [59] or potassium persulphate, used either alone or in combination with *N,N,N',N'*-tetramethylenediamine (TEMED). , Other photoinitiators used include benzophenone,[60] 2,2'-dimethoxy-2-phenylacetophenone, [61] benzoin ethyl ether and 2,4,6-trimethylbenzolphenylpho-sphinate. , O'Shannessy *et al.* compared photochemical and thermal initiation methods in the preparation of MIPs and a comparison of MIPs prepared by thermal and redox initiation has been performed by Haginaka *et al.* Another study of initiation methods by Sreenivasan compared **γ**-irradiation to thermal and photochemical methods.The utility of initiation by γ-irradiation [62,63] was also demonstrated by Biju *et al.* in the preparation of imprinted adsorbents for dysprosium ion which proved superior to those prepared by thermal means.[17] The use of iniferters such as benzyl-Af Af-diethyldithiocarbamate, which are photochemical quasi-living free radical polymerization initiators, has allowed the facile preparation of graft MIP layers on membranes, beads and surfaces.[64]

1.4.2 The effect of temperature and other polymerization conditions

The effect of polymerization temperature on MIP performance has been the subject of several studies.[65,66] While lower initiation temperatures may aid MIP preparation in some instances, the observation was made that the internal temperature within a monolith is much higher than the surroundings, due to the exothermal nature of the polymerization process. [57] High pressure has also been investigated for its effect on MIP synthesis, since it may favour associative processes such as formation of the pre-polymerization complex. Moderate beneficial effects of high pressure were seen. Spivak and Shea have surveyed reports of the imprinting of 9-ethyladenine and related the conditions of MIP formation, including temperature and cross-linker concentration, to MIP performance.

1.4.3. Cross-linkers

A large number of cross-linkers have been used in MIP studies, with divinylbenzene (DVB) and ethylene glycol dimethacrylate (EDMA) being the most commonly used. Wulff and co-workers compared a series of commercial and custom-made styrenic and methacrylate cross-linkers in some early studies, including pure isomers of DVB (the commercial material being a mixture of isomers). In their system EDMA was superior to DVB and its tetramethylene analogue in terms of the separation factor *(a),* shown by the MIPs. This was attributed to the combination of a short flexible linker and the rigidity and prochiral character of the methacrylate groups of EDMA. Other cross-linkers bearing more than two (meth) acrylate groups, such as trimethylolpropane trimethacrylate (TRIM), pentaerythritol triacrylate (PETRA),[67,68] and pentaerythritol tetraacrylate (PE-TEA),[67] have been shown to be superior to EDMA in some applications. Triethanolamine trimethacrylate and 1,2-fc-methacyloyloxyethyl benzenedicarboxylate have also been used as cross-linkers.1,3-Diisopropenylben-zene has been used as an alternative to DVB. Other cross-linkers investigated have included derivatives of amino acids, [57 ,69] hybrid cross-linkers, including vinyl ketones, a chiral cross-linker and a number of *bis*-acrylamides and methacrylamides.[70,71] Disulphide-linked b/s-acrylamides have been used as reversible crosslinks,[57], , and the use of flexible cross-linkers such as 1,4-butanediol dimethacrylate[71] and triethylene glycol dimethacrylate has been reported.

While methylene-to-acrylamide can be used to imprint in aqueous environments,[72] ethylene-to-acrylamide[73] and 1,4-diacryloyl piperazine , have higher solubility in water. Other studies have investigated the effect of the extent of cross-linking on site isolation[74] and recognition[75] in MIPs and Villamena and De la Cruz [57] have shown that DVB-based polymers show greater binding affinity for caffeine in aqueous media, compared to the equivalent EDMA- and TRIM-based polymers.

1.4.4. Porogen effects

The choice and quantity of porogenic solvent used in a polymerization recipe affects both the imprinting process and the physical state (pore structure, pore size distribution, swellability, toughness and morphology) of the MIP. While it is possible to dispense with a porogen when imprinting in the shell of sub-micron core-shell particles, higher capacities were seen in similar particles prepared with porogen. The preparation of *'in situ'* porous polymer rods for chromatography relies on specific porogen effects. Supercritical CO_2 has been proposed as an alternative porogen for MIP production.[76] The use of water in non-polar media has been shown to increase hydrophobic interactions; [77] conversely ionic interactions are enhanced through the presence of organic modifiers in aqueous porogens [78] between template and functional monomers.

1.5. Recognition and Binding

1.5.1 Template studies

The first published example from the group of Wulff involved enantioselective recognition of glyceric acid in covalently imprinted polymers. Since then a number of studies have investigated the effect of polymer and template structure on the binding properties of covalent and non-covalent MIPs. Covalent imprinting of sugars using boronic acid derivatives appears to be dependent on the spatial distribution of functional groups rather than absolute structure, implied by cross-reactivity of a D-galactose-im-printed polymer with L-fructose and vice-versa. This is reflected in the ability of Schiff's base templates to immobilize functional groups at precise distances in a cross-linked polymer or on a silica surface.

Template effects in covalently imprinted polymers were also investigated by Shea and Sasaki using the ketal approach, and the extent of one- and two-point binding in similar materials has also been investigated. Alexander et al. showed that binding to a boronophthalide-based covalently imprinted polymer was consistent with the template structure by the selective derivatization of unprotected hydroxyl groups on analogues of the template sterols.[79] Template removal is an issue in non-covalent MIPs used for SPE in ultra-trace analysis; in particular slow template bleeding can occur which can interfere with analyte detection. A study by Ellwanger et al. compared methods for complete template removal to minimize template bleed.[80] The use of analogues or 'dummy templates'[81] may help to circumvent these problems. The effect of extremely high monomer to template ratios has been studied; in both cases significant imprinting effects were seen with very low template concentrations. The effect of template size on the selectivity of MIPs has been studied,[82] as has the effect of intramolecular H-bonding in the template on its imprint.[83] Allender et al. have attempted to explain the observed cross-reactivities in binding to MIPs for amino acid derivatives in terms of the ligand structures, and Spivak and Campbell have performed a similar study on amine-imprinted MIPs.[84] The effect of template structure and acidity has been compared in the imprinting of nitrophenol and hydroxybenzoic acid isomers.[85] A study by Yu and Mosbach compared the performance of acrylamide-based MIPs prepared with a range of N-protected amino acids. Template-template association has also been reported in the case of nicotine imprinting, and template-like functional monomers have also been employed in the case of cholesterol imprinting.A physicochemical study of the origin of the imprinting effects in ion-templated microspheres has been reported by Miyajima et al. D'Oleo et al. have reported an 'imprinted' material prepared without a template[86] using crosslinks within a gel to pre-organize a calcium-binding site.

1.5.2. Solvent effects in binding

The general observation that MIPs perform better in recognition studies performed in the same solvent as that used in MIP synthesis has been reported. However, MIPs can show effective recognition in solvents other than that used as porogen, including aqueous buffers; in this case a switch in recognition mechanism from H-bonding to hydrophobic recognition can be demonstrated by a loss of recognition in intermediate aqueous–organic mixtures.

The effect of organic modifiers, such as acetic acid, on binding to MIPs in HPLC has been studied; they function by reducing non-specific interactions with both MIP and control. The use of surfactants as modifiers in aqueous-based recognition studies and in SPE and chromatography has also been reported.[87]

1.5.3. Selection approaches to MIP optimization

The application of high-throughput synthesis techniques to MIP preparation and screening was developed independently by the groups of Takeuchi [88] and Sellergren.[89] These techniques have allowed a range of MIP monomer and/or solvent compositions to be synthesized for comparison and optimization for binding properties[90] or application.[91]

1.5.4. Chemical and physical post-treatment of MIPs

Chemical modification of functional groups within the recognition site of MIPs has been used to demonstrate the contribution of the functional monomers to recognition, by inducing a loss of function in non-covalent, semi-covalent and crystal-imprinted[92] polymers. This was achieved by reaction with diazomethane, acyl chlorides and acidified metha-nol respectively. A similar approach has been used in the presence of bound template to modify the binding site distribution in favour of the higher affinity sites by selective poisoning of the low-affinity sites.[93] Esterification with blocking agents of different sizes has also been demonstrated to modify the binding properties of semi-covalently imprinted polymers.[94] The use of chiral ligands as poisons for imprinted catalysts has also been attempted.[95] Modification of the binding properties of imprinted silicas has been demonstrated by the thermal decomposition of carbamate templates and quenching of the silica-bound isocyanate group with water or an alcohol (ethylene glycol) to give alternative functional groups in the template site.[96] Post-oxidation of thiol groups derived from disulphide-linked templates has been used to modify MIPs and the treatment of polymers in which the ester template has been cleaved by hydride reduction resulted in polymer-bound hydride reagents for stereo- and regioselective reduction of ketones.The effect of thermal annealing on the recognition properties of MIPs has also been studied.

1.6. Thermodynamics, Physical Characterization and Modelling

Thermodynamic aspects, including modelling and mathematical analyses of equilibria and binding site distribution, can be divided according the stage of preparation of the MIP that is being considered. These broadly fall into the categories of: (i) the pre-polymerization complex, (ii) formation of the imprinted network and (iii) the ligand binding properties of the resultant MIP. The following sub-sections will survey publications in these areas in turn.

1.6.1. Thermodynamic aspects and modelling of the pre-polymerization complex

The establishment of complexes in the mixture of monomers and template prior to polymerization in non-covalent molecular imprinting is the dominant theory of the basis for imprinting in these materials. The theory is backed by both thermodynamic arguments and experimental studies. Nicholls *et al.* have discussed the contributions of individual enthalpic terms and entropic factors to the free energy of binding to MIPs and their consequence of the design of imprinted polymers, template and monomer selection and solvent effects.[97] The speciation of individual monomers-template complexes was modelled by Sellergren *et al.,* using binding constants determined for their template, L-phenylalanine ani-lide. A more extensive theoretical model of the speciation with ligands of different affinity for the template and the consequence for MIP selectivity was published by Whitcombe *et al.* who used NMR titration to measure a typical association constant encountered in non-covalent imprinting. Computer modelling has been proposed as a tool for predicting ligand-receptor interactions in MIPs for desulphurization of fuels and the modelling of the interactions between template molecules and a virtual library of functional monomers was proposed by the group of Piletsky as a means of identifying candidate monomers for MIP synthesis. The energy of complexes was minimized during a simulated annealing process using molecular dynamics. The approach was successfully used in the design of MIPs for ephedrine, creatinine and the cyanobac-terial toxin, microcystin-LR.[98] Computer modelling of the pre-polymerization complex has also been employed to predict the chromatographic behaviour of MIP stationary phases by Wu *et al.*[99]

The order of the calculated binding constant was reflected in the capacity factors of the corresponding MIP columns for a series of aromatic templates.

1.6.2. Spectroscopic studies of the pre-polymerization complex

Direct observation of complexation between monomers and template molecules or their analogues has been observed by changes in spectroscopic properties of the mixtures. NMR methods and UV spectrophotometry are the most popular; however, FT-IR and x-ray crystallography have also been applied to the problem. Changes in the chemical shift values of key residues in NMR titration experiments have been used to establish the stoichiometry of complexes (Job's method), [57] or the association constants between monomer and template. NMR titrations of MAA with atrazine, 2-aminopyridine, 4-L-phenylala-nylamino-pyridine, biotin and ephedrine [57] have been reported. Acetic acid and deuteropyridine were also used in an NMR titration with 17-a-ethynylyestradiol as substitutes for MAA and 4-vinylpyridine respectively. In addition to chemical shift changes, line widths of NMR signals have also been used to infer complex formation. NMR measurements, including NOE, were used by Lepisto and Sellergren to show the importance of template conformation on the specificity of an imprinted polymer. A problem with fully modelling the environment in the pre-polymerization mixture is the presence of large quantities of cross-linker, which may interfere with the NMR experiment. This may not prove to be a limitation when complex formation can be followed by UV spectroscopy, which can also be performed in the presence of EDMA.[100] Monomer analogues (acetic acid for MAA and trifluoroacetic acid for trifluor-omethylacrylic acid) can also be used in UV titration with similar results to the monomers[101] and provide a useful model system. While isolated templates are usually assumed, template-template association has been observed and probed using a polymerizable analogue of the template.[102] NMR measurements have also been followed during the polymerization of typical MIP formulations and show no apparent change in the nature of complexation for as long as the signals can be observed, suggesting that the template–monomers complexes persist during the polymerization process,[103] although differences between the solution and solid states have been observed in other systems.[104] Infra-red spectroscopy has also been used to probe monomer–template interactions, as an aid to optimization of MIP properties.[105]

1.6.3. Modelling polymer formation in the presence of templates

Srebnik and Lev[106] used mean-field theory to simulate the effect of simply modelled templates on imprinted networks with different degrees of cross-linking. Their conclusions support the observation that a rigid network is necessary for effective imprinting. The same approach was applied to the modelling of inorganic gels308 including a molecular dynamic simulation of the gelation process.

The group of Tanaka also used a computer modelling approach to show that polymerization, by forming 'bonds' between 'monomers' at the vertices of a 3-dimensional matrix in the presence of a template, can result in a polymer chain with a probabilistic tendency to renature to a binding conformation for the template, given suitable energetics of interaction between components of the system.[107] The model has also been extended to predictions of the phase diagrams of linear imprinted polymer sequences.[108,109] While the discussions in these papers relate to protein folding and analogous processes in which context 'imprinting' has a more general meaning, taking into consideration all of the interactions between components of uncross-linked polymers and their effect on conformation, the authors themselves point out the similarity between their approach and that of Wulff and Mosbach.[110] This theory has led to a number of reports of lightly and/or reversibly cross-linked gel formulations in which imprinting through groups of at least two interactions of functional monomers with templates (Ca^{2+}, Pb^{2+}, pyrenesulfonic acids) give rise to a higher binding capacity than similarly prepared random (non-imprinted) gels in which frustrations of the polymer chain prevent multiple interaction with the target, with a reduced binding capacity as the result.[3,4,111] The template adsorption could be further increased by a 'post-imprinting' step where reversible cross-links were reformed in the presence of template. The theoretical basis of the 'Tanaka approach' is set forth in a recent paper.[112] An approach to a theoretical description of adsorption in poly-disperse templated porous material has also been developed based upon the Ornstein-Zernicke equations.[113]

1.6.4. Characterizing the binding sites and their distribution

The analysis of the binding properties of MIPs is based on methods developed for characterizing antibodies and other biological receptors. Fitting of binding isotherms (obtained by batch methods [114] or frontal analysis of chromatographic data)[115] to a Langmuir or multi- (commonly bi-) Langmuir model has commonly been performed, either using curve-fitting software to analyse the isotherm, or by a graphical method such as a Scatchard plot. The realization that the Langmuir isotherm is not a very precise description of the binding behaviour of non-covalently imprinted MIPs led to the investigation of alternative binding models such as the Freundlich[116–117] and Langmuir– Freundlich[118,119] isotherms. Umpleby et al. also proposed the affinity spectrum as a general description of the distribution of binding site affinity in MIPs,[120] and used this analysis to demonstrate that selective chemical modification of binding sites could alter the distribution in favour of higher affinity sites. An earlier method of plotting the distribution of sites in terms of their chiral discriminating ability was published by Wulff et al. for covalent MIPs. Kim and Spivak have used a method based on the Freundlich isotherm to investigate the effect of template concentration on the yield and stoichiometry of non-covalently imprinted sites. Measurements of the optical activity of covalent MIPs after template cleavage have demonstrated the chiral induction in the cross-linked structure due to the template.

1.6.5. Physical methods of characterizing the rebinding event

Both ^{13}C CP-MAS solid-state NMR and FT–IR spectroscopy have been used to probe the binding in covalently imprinted polymers using ketal formation. A similar approach was used by Katz and Davis to investigate silica imprinted by a semi-covalent method, in addition fluorescent probes, porosimetry and FT–IR were also used to characterize the imprinted sites. A study by Sasaki and Alam used ^{31}P and ^{29}Si MAS NMR to characterize one- and two-point binding in a guanidine-functionalized imprinted silica NMR methods have also been used to study the structure of poly(styrenes) cross-linked with crown ether groups in the presence of organic cation templates. Isothermal batch and stirred microcalorimetric investigations have also been performed on covalent and non-covalently imprinted[121,122] polymer to detect the binding event.

Electrochemical measurements and Raman spectro-scopy have been used to characterize recognition sites in imprinted monolayers, cyclic voltammetry has been used to investigated the factors involved in rebinding of Cu^{2+} to a metal-imprinted polymer and steady-state and time-resolved fluorescence measurements have been used to monitor the specificity and selectivity of fluorescent MIPs for template.[123] Fluorescence techniques have also been discussed for probing molecular interactions in MIPs. Surface-enhanced Raman scattering (SERS) has been used to monitor uptake and release by MIPs.[124]

1.7. Parameters Involved in Mmolecular Rrecognition Events

Evidence for shape selectivity in MIPs synthesized via non-covalent interactions has been found using molecular probes of different sizes. In the self-assembly approach, the cross-linker may be a third component influencing the properties of the formed pre-polymerization complexes. The binding constants of different possible complex configurations ultimately determine their ability to 'survive' the polymerization process, which results in the formation of binding pockets or binding sites. In consequence, it is expected that polymers with a heterogeneous binding site distribution will be formed with affinity distributions ranging from binding sites with high affinity for the template, to nonspecific binding to the cross-linked polymer matrix, including multi-site recognition (multimers). Results on studies related to the nature of recognition in MIPs are widely contradictive and range from indications towards recognition taking place in cavities and not by interaction with residual template molecules, to recognition due to residual template interaction.

Tablo 1.1 Parameters contributing to molecular recognition

Parameters contributing to molecular recognition
Size
Shape (conformation, configuration)
Functionality (shape + functionality → chirality)
Electronic properties of binding analyte
Electronic properties of surrounding polymer matrix (polarity, functionalities)
Reactivity of binding site (ionic interactions)
Accessibility of binding site (polymer porosity, density)

1.7.1. Molecular interactions involved in non-covalent imprinting

The main non-covalent interactions responsible for molecular recognition in biomimetic systems are hydrogen bonding, ion-pairing, and π-π interactions (see Table 3). Furthermore, Coulombic attraction, charge transfer, induction, dispersion, and exchange-repulsion contribute to the complex formation. The driving forces of ion-pairing interactions (ion-ion, dipole-ion, dipole-dipole) are Coulombic interactions. Hydrogen bonding is a strong interaction playing an important role in naturally occurring non-covalent interactions. Complexes based on hydrogen bonding typically exhibit comparatively high stability constants. Table 2 gives examples of hydrogen bonding donor and acceptor groups.

Table 1.2 Hydrogen bonding donor and acceptor groups.

Donor	Acceptor
O − H	O ═ P
N − H	O ═ S
N^{+} − H	O ═ C
S − H	-N═ or -O-
C − H	S═ C

These interactions are favored in weakly polar aprotic solvents such as acetonitrile. In contrast, more polar protic solvents support interactions such as metal-ion coordination of the template molecule. Comparatively weak electrostatic interactions such as π-π stacking may occur between aromatic rings in polar solvents such as water and methanol. Hydrophobic interactions are only facilitated in highly polar solvents or solvent mixtures such as water/methanol.

Table 1.3 Types and estimated bond energies of non-covalent interactions.

Bond type	Bond energy [8,9,10] [kJ/mol]	Relative strength
Hydrogen bond	20[8] 4-60[9] 2-5[10]	weak/medium
Hydrophobic effects	1-3[8]	weak
Ion-ion (1/r)	250[8] 100-350[9]	strong
Dipole-ion ($1/r^2$)	15[8]	weak
Dipole-dipole ($1/r^3$)	2[8] 5-50[9]	weak/medium
π-π stacking	0-50[9]	weak/medium
Dispersion (London) ($1/r^6$) (attractive van der	2[8] <5[9]	weak
Cation-π	5-80[9]	medium

The wide variety of possible interactions implies that molecular recognition of a guest molecule may be dominated by one mode of molecular interaction or controlled by a combination of different recognition mechanisms, which are enabled or disabled depending on the polarity of the selected protic or aprotic porogen. In general, the combination of two or more interaction modes can be expected.

1.8. Sensors Involving Molecularly Imprinted Polymers

Chemical and biosensors are of increasing interest due to their potential applications in clinical diagnostics, environmental analysis, food analysis and pollution monitoring as well as the detection of illicit drugs, genotoxicity and chemical warfare agents. The central part of a chemical or biosensor is the recognition element, which is in close contact with an interrogative transducer.

The recognition element is responsible for specifically recognizing and binding the target analyte in an often complex sample. Biosensors rely on biological entities such as antibodies, enzymes, receptors or whole cells as recognition elements. The possibility of tailor made highly selective, artificial receptors at low cost, with good mechanical, thermal and chemical properties has paved the way for the development of a new generation of chemical sensors, using novel synthetic materials as recognition elements. One technique that is being increasingly adopted is molecular imprinting in synthetic polymers.

Until recently, most of the published accounts for sensors have described phenomena that may lead to a sensing device but not the development of actual devices. The difficulty in making sensors with imprinted polymers resides in finding a sensitive means by which chemical recognition can be coupled to signal transduction. The two major methods used for signal transduction in ionic sensors are based on electrochemical and spectroscopic properties. The production of polymers exhibiting selective binding of a specific cation involves the formation of cavities equipped with complexing agents so arranged as to match the charge, coordination number, coordination geometry and size of the target cation. The combination of imprinting and transduction selectivities can result in sensors that exclusively recognize the target analytes and not the interfering species .

1.8.1. Fluorescence-based sensing devices

Fluorescence spectroscopic sensing represents an attractive means of creating an effective chemosensor, due to ease of use and detection of sub-micromolar concentrations; thus,the incorporation of chromophoric reporter molecules into molecular imprinting sensor designs has been researched to a considerable extent.[125] As molecularly imprinted materials are inherently versatile, a variety of methods have been employed to attain optical transduction of specific binding events via fluorimetry. One of the first reported techniques was that of Piletsky et al.[126] Using sialic acid as template, a covalently-bound monomer–template complex was created with vinylphenylboronic acid. After preparation of the imprinted polymer, it was further treated with a fluorescent agent (o-phthaleic dialdehyde and mercaptoethanol).

The authors noted an increase in polymer fluorescence intensity upon rebinding of the template molecule, which they attributed to an increase in polymeric permeability; detection of sialic acid in the micromolar concentration range was achieved. Piletsky and co-workers [127] also examined the use of competitive rebinding of a fluorescent compound and an unlabelled template molecule, in sensors specific for a selection of triazine herbicides. A fluorescent compound analogous in structure to the triazine compounds (5-(4,6-dichlorotriazinyl)-aminofluorescein) was used as the competing reporter compound. Detection of analyte in the concentration range of 0.01mMup to 100mM was reported, and sensor response indicated the presence of two distinct classes of binding site, of differing affinities. The method of competitive displacement has also been extended to tracking enantioselective MIP/analyte binding events,[127] and development of a flow-through assay for the antibiotic chloramphenicol.Rachkov and colleagues similarly used a competitive displacement system for determination of estradiol; however, as the template here is intrinsically fluorescent, direct measurement of the analyte concentration could also be made. A commonly used method of introducing fluorescence transduction of binding events to a MIP is derivatization of functional monomers to include a fluorescent moiety, such that when analyte rebinds to a specific cavity wherein these modified monomers are located, resultant changes in the electronic properties of the monomers produce a fluorescent signal. Rathbone and co-workers[128] synthesized a selection of monomers bearing fluorescent substituents (such as coumarin and acrylamidopyridine), which effectively reported rebinding of template when included in an imprinted polymer. A similar approach yielded MIPs for the biologically important compound cyclic guanosine monophosphate. [129] The detection of carbohydrates upon rebinding to a MIP was accomplished via integration of an anthraceneboronic acid conjugate monomer into a MIP, as described by Gao et al.[130] The same research group has also developed a sensing method for L-tryptophan, via attachment of a dansyl moiety to the functional monomer, methacrylic acid. However, as the shift in fluorescence signal of the MIP upon rebinding was inadequate for use in a sensor, the authors included a quenching compound, p-nitrobenzaldehyde. In this embodiment, template competed with quencher and increased the fluorescent signal dramatically upon rebinding, creating a more effective sensor. Detection of single-digit micromolar concentrations of the amino acid could be achieved.

Similarly, quenching using iodide and acrylamide has been examined in ricinimprinted organosilanes.[131] A fibre-optic detection system for L-phenylalanine was developed by Kriz et al.[132,133] via fluorescent tagging of the template, in this case, with a dansyl moiety. Fibre-optic-based fluorescence has also been exploited by Hart. As an alternative to tagging of the monomer, Chow et al. developed a MIP specific for D,L-homocysteine tagged with a fluorescent agent; it was found that this MIP specifically enhanced the rate of the D,L-homocysteine derivatization reaction. Fluorescent detection of aqueous adenosine 3':5'-cyclic monophosphate (cAMP), a molecule of biological significance, was examined by Turkewitsch et al.[134] via incorporation of a fluorescent dye (trans- 4-[p-(N,N-dimethylamino)styryl]-N-vinylbenzylpyridinium chloride) into the binding sites. Quenching of the dye was observed upon rebinding of the templated cAMP molecule to the MIP, but none was observed in the presence of structural analogues. Binding constants for the template molecule to the polymer were of the order of $10^{-5}M^{-1}$. Further research [135] on this system, using time-resolved fluorescence decay analysis, allowed comparison between template-fluorosensor interactions in solution and inside MIP binding sites. The analysis pointed to the existence of two kinds of binding sites in the MIP the first class of sites accessible to solvent, and the second of restricted access or enclosed in the polymer matrix. Fluorescence studies may thus reveal information about the binding sites via changes in the photophysical properties of the reporter compound. The incorporation of a fluorescent reporter into imprinted binding sites is also notable for the levels of detection achievable in some cases, as low as parts per trillion, as in the sol-gel imprint of the herbicide DDT by Grahamet al. Imprinting of compounds which have an inherent fluorescence offers even greater simplicity in the design of sensors, as it permits direct fluorescence measurement. This was demonstrated notably by Matsui and coworkers, who imprinted cinchonidine and cinchonine using trifluoromethacrylic acid as functional monomer. A characteristic shift in the fluorescence signal was observed upon binding of the alkaloids to the MIP, pointing to a possible protonation of the alkaloids as the source of the fluorescence shift. The intrinsic fluorescent properties of flavones have also been exploited to create a MIP-based fluorosensor. Using flavonol (3-hydroxyflavone) as template molecule, Suarez-Rodrıguez and Dıaz-Garcıa[136,137] integrated a MIP into a flow-through sensor with a detection limit of $5x10^{-8}$ M, and a linear range of $5x10^{-8}$ up to 10^{-5} M.

Using an exchange resin to immobilize template, Ferna´dez-Sa´nchez et al. created a fluorescence-based flowthrough sensor for propranolol. The fluorescent organic compounds fluorescein and N-acetyltryptophanamide were used in the preparation of molecularly imprinted silanes,[138] such that direct fluorescence measurements could be made to investigate re-occupancy of these polymeric materials. Sub-micromolar quantities of template could be detected, and again two classes of binding sites, of differing affinities were observed. In all cases here, fluorescent analytes permitted facile development of a sensor. One other area which has been examined is that of metal ion recognition and use of metallic compounds for the purposes of generating a fluorescent signal upon specific binding. Aluminium is considered an important analyte due to its presence in drinking water; by imprinting an aluminium (III) morin chelate, Al-Kindy et al.[27] developed an aluminium-specific sensor. This sensor again exploits the inherent fluorescence of a flavonoid-type compound (similar to flavonol [136]), with recognition depending on chelate stoichiometry, as well as the nature of and ionic radius of the metal ion. A limit of detection of 1 $mgmL^{-1}$ was established with this flow-through sensor. A fluorimetric MIP sensor has been designed by Güney et al for lead ions,[21] using a combination of methacrylic acid and the fluorescent 9-vinylcarbazole as functional monomers. Formation of complexes between the imprinted polymer and lead ions resulted in quenching of the fluorescence of the carbazole reporter molecule. Lead ions in the range of 10^{-6} up to 10^{-2}M could be determined. Lead was also detected via a fluorescent polymer developed by Zeng et al. Tong and co-workers[42] integrated a zincbased porphyrin compound as fluorescent reporter/functional monomer in an MIP sensor specific for histamine; it was found that use of a mixture of both this compound and methacrylic acid resulted in MIPs of high specificity. Saturation was observed at histamine concentrations of above 10^{-3} M.

1.8.2. Optical sensors

While fluorescence-based sensing approaches offer high levels of sensitivity, optical sensing methods have the significant advantage of conceptual simplicity and do not require an expensive method of detection. Relatively few analytes are conducive to optical detection however, and typically either a template derivatization or a dye displacement technique is required.

Levi et al.[139] developed a sensor selective for the antibiotic chloramphenicol by creating a chloramphenicol–methyl red dye conjugate, which was displaced from an imprinted polymer by chloramphenicol, resulting in a measurable change in absorbance at a high wavelength (460 nm). A linear response was observed in the concentration range 3–1000 $mgmL^{-1}$. Methyl red itself was imprinted in a study by Liang and co-workers to examine what effect imprinting has on the pKa of an indicator. A different approach was adopted by Nopper et al. measurements via reflective interference spectroscopy permitted design of a molecularly imprinted chiral chemosensor.

1.9. Fluorescence Spectroscopy

Fluorescence spectroscopy is one of the most widely used spectroscopic techniques in the fields of biochemistry and molecular biophysics today. Although fluorescence measurements do not provide detailed structural information, the technique has become quite popular because of its acute sensitivity to changes in the structural and dynamic properties of biomolecules and biomolecular complexes. Like most biophysical techniques, fluorescence spectroscopic studies can be carried out at many levels ranging from simple measurement of steady-state emission intensity to quite sophisticated time-resolved studies. The information content increases dramatically as various fluorescence observables are time resolved and combined in global analyses of the phenomena of interest. Nonetheless, quite a good deal of information is available from steady-state measurements for which the requirements in instrumentation are quite modest. Consequently, steady-state fluorometers are routinely used to measure complexation and conformational phenomena of biological molecules.

1.9.1. Jablonski diagram.

Processes which occur between the absorption and emission of light are usually illustrated by a Jablonski diagram. A typical Jablonski diagram is shown in Figure 1.2. The ground, first and second electronic states are depicted by S0, S1 and S2, respectively. At each of these electronic energy levels the fluorophores can exist in a number of vibrational energy levels (denoted by 0, 1, 2, etc.).

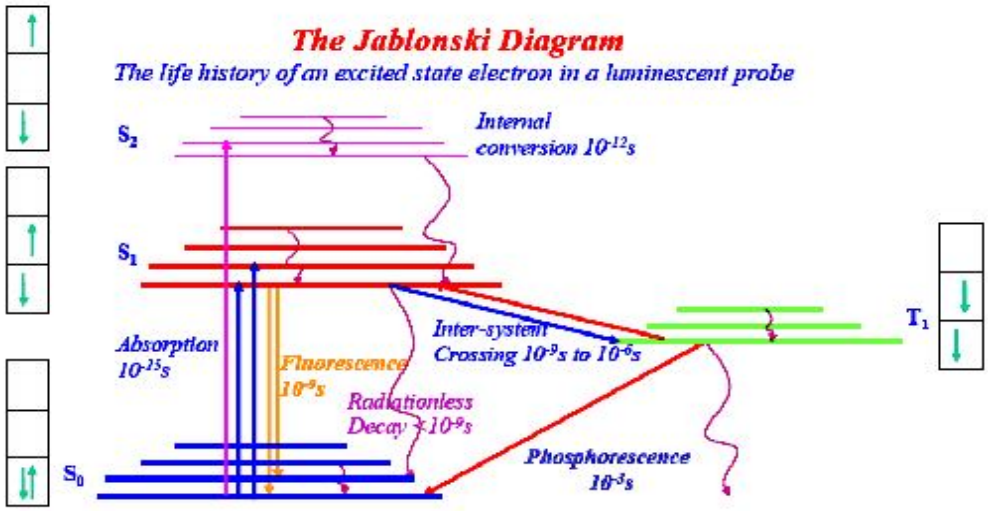

Figure 1.2 Jablonski Energy Diagram

Transitions between states are depicted as vertical lines to illustrate the instantaneous nature of light absorption. Transitions occur in about 10^{-15} seconds, a time too short for significant displacement of nuclei. (Franck-Condon principle).

Following light absorption, several processes usually occur:

1.9.1.a. Fluorescence.

Fluorescence is emission light from singlet-excited states, in which the electron in the excited orbital is paired (of opposite sign) to the second electron in the ground-state orbital. Return to the ground state is spin-allowed and occurs rapidly by emission of a photon. These emission rates of fluorescence are typically 10^8 s^{-1}, so that a typical fluorescence lifetime is near 10 ns. Fluorescence spectral data are generally presented as emission spectra. Emission spectra vary widely and are dependent upon the chemical structure of the fluorophore and the solvent in which it is dissolved.

A fluorophore is usually excited to some higher vibrational level of either S_1 or S_2. With a few rare exceptions, molecules in condensed phases rapidly relax to the lowest vibrational level of S_1. This process, called internal conversion, is nonradiative and takes place in 10^{-12} seconds or less. Return to the ground state occurs to a higher excited vibrational ground-state level, which then quickly reaches thermal equilibrium. An interesting consequence of emission to a higher vibrational ground state is that the emission spectrum is typically a mirror image of the absorption spectrum of the S_0 to S_1 transition.

1.9.1.b. Intersystem crossing.

Molecules in the S_1 state can also undergo a spin conversion to the first triplet state, T_1. Emission from T_1 is termed phosphorescence and is generally shifted to longer wavelengths (lower energy) relative to fluorescence. Transition from the T_1 to the singlet ground state is forbidden, and as a result, the rate constants for triplet emission are several orders of magnitude smaller than those for fluorescence.

1.9.2. Characteristics of fluorescence emission.

1.9.2.a. Stokes Shift

The energy of emission is typically less than that of absorption. Thus, fluorescence occurs at longer wavelengths.. The phenomenon is known as the Stokes Shift and can be caused by:

a.) Energy losses due to relaxation to ground vibrational states.

b) Solvent effects

c) Excited state reactions

d) Complexformation

e) Energy transfer

1.9.2.b. Kasha's rule

Emission spectra are typically independent of the excitation wavelength.Upon excitation to higher electronic and vibrational levels, the excess energy is quickly dissipated, leaving the fluorophore in the lowest vibrational level of S_1. It is from this position that the photon will be emitted. Exceptions to this rule indicate a different geometric arrangement of nuclei in the excited state as compared to the ground state. Nuclear arrangements can occur prior to mission because of the relatively long lifetime of the S_1 state, which allows time for motion following the instantaneous process of absorption.

1.9.2.c. Mirror image rule.

The emission is the mirror image of the $S_0 \rightarrow S_1$ absorption, not of the total absorption spectrum. This is a result of the same transitions being involved in both absorption and emission and the similarities of the vibrational levels of S0 and S1. In

many molecules these energy levels are not significantly altered by the different electronic distributions of S_0 and S_1. If a particular transition probability between the zeroth and second vibrational levels is largest in absorption, the reciprocal transition is also most probable in emission.

1.9.3. Fluorescence quenching

Fluorescence quenching refers to any process that decreases the fluorescence intensity of a sample. There are a wide variety of quenching processes that include excited state reactions, molecular rearrangements, ground state complex formation, and energy transfer. Quenching experiments can be used to determine the accessibility of quencher to a fluorophore, monitor conformational changes, monitor association reactions of the fluorescence of one of the reactants changes upon binding. There are two basic types of quenching: static and dynamic (collisional). Both types require an interaction between the fluorophore and quencher. In the case of dynamic quenching the quencher must diffuse to the fluorophore during the lifetime of the excited state. Upon contact the fluorophore returns to the ground state without emission of a photon. In the case of state quenching a complex forms between the flurophore and the quencher, and this complex is non-fluorescent. The formatin of this complex does not rely upon population of the exited state. We will consider them independently.

1.9.3.a. Collisional quenching.

Collisional quenching occurs when the excited-state fluorophore is deactivated by contact with some other molecule in solution, which is called the quencher. The molecules are not chemically altered in the process. For collisional quenching, the decrease in intensity is described by the ratio of the fluorescence in the absence of quenching to the presence of quencher by the Stern-Volmer equation:

$$\frac{F_0}{F} = 1 + K_{SV}[Q] = 1 + k_q \tau_0 [Q]$$

where F_0 and F are the observed fluorescence in the absence and presence of quencher, K is the Stern-Volmer quenching constant, $k_q is$ the bimolecular quenching constant, T_0 is the lifetime in the absence of quencher, and *[Q]* is the quencher concentration. The Stern-Volmer constant is sometimes abbreviated as K_{SV} or even as

K_D. The use of the K_D abbreviation seems very unwise in my opinion, since it could lead to confusion. Thus, the reader should be aware of the context in which this term is being used.

1.9..3.b. Mechanisms of quenching.

The accessibility of fluorophores to quenchers can be used to determine the location of fluorescent probes on macromolecules, and a wide variety of molecules can act as collisional quenchers, and the mechanism varies with the fluorophore-quencher pair. Common substances used for quenching are halides: bromide and iodide (I^-), oxygen and acrylamide.

Mechanisms of quenching are subject to debate. In the case of oxygen, which is paramagnetic, it is thought that it may cause the fluorophore to undergo intersystem crossing to the triplet state. In fluid solutions these long-lived triplet states decay before phosphorescence can occur. Halides such as iodine and bromine are also thought to cause intersystem crossing to the excited triplet state, promoted by spin-orbit coupling of the excited state fluorophore and the halogen. Other quenchers, such as Cu^{2+}, Pb^{2+} and Cd^{2+} are though to cause the donation of an electron from the fluorophore in the excited state.

1.9.3.c. Stern-Volmer plot

Because of the linear dependence quenching data are usually presented as plots of F_0/F versus $[Q]$. This plot should yield an intercept of unity on the y-axis and a slope equal to K_{SV}. An example of such a plot is shown in Figure 5. It is useful to note that $1/K_{SV}$ is the quencher concentration at which $F_0/F = 2$, or 50% of the intensity is quenched. A linear Stern-Volmer plot is generally indicative of a single class of fluorophores that are all equally accessible to the quencher. If two fluorophore populations are present, and one class is not accessible to quencher, then the Stern-Volmer plots deviate from linearity toward the x-axis (downward). This result is frequently found for the quenching of tryptophan fluorescence in proteins by polar or charged quenchers.

1.9.3.d. Static quenching

Static quenching involves the formation of a complex between the quencher and fluorophore that does not rely on diffusion in the excited state. The dependence of the

fluorescence intensity upon quencher concentration for static quenching is derived by consideration of the association constant for complex formation:

$$K_s = \frac{[FQ]}{[F][Q]}$$

where K_S is the fluorophore-quencher association constant, [FQ] is the concentration of the complex, [F] is the concentration of the uncomplexed fluorophore, and [Q] is the concentration of quencher. Since the total concentration of the fluorophore, FT is given by $[F]_T = [F] + [FQ]$, the static quenching constant can be written as:

$$K_s = \frac{[F]_T - [F]}{[F][Q]} = \frac{[F]_T}{[F][Q]} - \frac{1}{[Q]}$$

which rearranges to:

By recognizing the fluorescence signal in the absence of quencher, F_0 would correspond to the total concentration of fluorophore, one can substitute the fluorescence intensities F_0 and F for the total and free concentrations $[F]_T$ and [F], respectively to obtain:

$$\frac{F_0}{F} = 1 + K_s[Q]$$

which you will recognize is exactly the same linear equation we used for dynamic quenching.

1.9.3.e. Both static and dynamic quenching can have a linear Stern-Volmer plot

Static quenching also gives a linear Stern-Volmer plot and so static and dynamic are distinguished from each other by their differing dependences on temperature, viscosity or lifetime measurements. An increase in temperature leads to an increased in the diffusion constant of quencher and will generally lead to an increase in collisional quenching. In contrast, an increase in temperature will generally lead to a decrease in the binding constant of quencher for fluorophore and will result in a decrease in quenching for a static quencher.

2. EXPERIMENTAL

2.1. Materials

Methacrylic acid (MAA), 2,2-azobisisobutyronitrile(AIBN), ethyleneglycol dimethacrylate (EGDM), vinylimidazole (VIm) and 9-vinylcarbazole (VCz) were obtained from Aldrich. Benzofuran chalcone methacrylamide (BCM) was provided by şenkal group at ITU. Lead methacrylate ($PbMAA_2$) was obtained from Alfa-easer. The organic solvents were of HPLC grade (Aldrich).

2.2. Structure of Fluorescent Monomers Used in Synthesis of Polymeric Materials

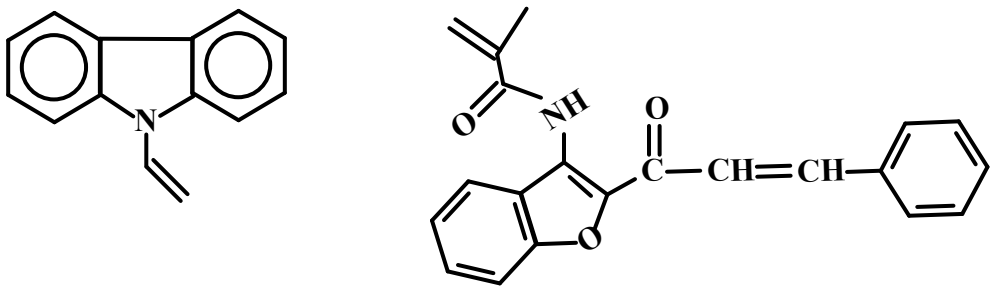

VCz **BCM**

Figure 2.1 : The chemical structure of VCz and BCM

2.3. Synthesis of Lead-ion Imprinted Sensor Containing VCz

Lead ion imprinted sensor consisting of VCz and MAA was prepared using 50mM of lead methacrylate ($PbMAA_2$), 50 mM of VCz, 2M of ethyleneglycol dimethacrylate (EGDMA) and 20 mM of 2,2'-azobisisobutyronitrile (AIBN) in 1,4-dioxane as a solvent. Sensor was prepared by free radical polymerization of VCz and $PbMAA_2$ with cross-linker EGDMA in dioxane.

After the addition of AIBN initiator, the solution was immediately transferred into narrowly spaced Teflon mould covered with glass plates to obtain a slab polymeric material. The solution was then degassed under vacuum. The polymerization was carried out at 60 °C during 24 h.

2.2.1. Removal of the lead-ion from the synthesized polymers

The slab polymeric materials were taken out of the glass plates and washed consecutively with deionized water, 100 mM HC1 and 100 mM NaOH solution, for 2 days in each medium that was replaced each 12 h, to remove unreacted molecules and the template, Pb^{2+}, ions. The slab materials with a thickness of 0.9 mm were removed from the solution and dried for 4 days under vacuum at room temperature. Then the polymeric material was used to determine the concentration of the metal ions in aqueous solutions by monitoring the fluorescence intensity of the carbozole groups quenched upon the complex formation with the lead ions diffused into the resin.

Nonimprinted polymer was also synthesized at the same reaction conditions. But MAA was used as a functional monomer in the preparation of random polymer instead of using $PbMAA_2$. Meanwhile same washing procedure was applied to the randomly synthesized polymeric material.

2.3. Synthesis of Iron-ion Imprinted Sensor with VCz

Iron-ion imprinted polymeric resins were synthesized using a molar ratio of 1:1:40 ($FeSO_4.7H_2O$: MMA : EGDMA). The complex of iron-ion with VCz was solublized in DMSO as solvent and polymerized with the functional monomer (MMA) and cross-linking monomer (EGDMA) using AIBN as initiator. Then the solution was transferred into glass tupe with 4 mm diameter covered with Teflon band. The polymerization was carried out at 60 °C during 24 h after the solution was degassed under vacuum.

2.3.1. Removal of the iron-ion from the synthesized polymers

The iron-ions were leached from the above synthesized polymeric sensor materials by stirring with 100 ml of 50 % (v/v) HCl for 18 h. The resultant resin materials, shape of cylindrical obtained after washing with water were dried in an vacuum desiccater at room temperature to get iron-ion imprinted resin for possible recognation of iron-ions from dilute aqueous solutions.

2.3.2. Synthesis of the control polymer particles

The synthesis of the corresponding control polymeric resins (nonimprinted sensor) were prepared under the same conditions as that of the iron-ion imprinted sensor except the imprint iron metal-ions. The control polymers were also subjected to same pretreatments as that of the iron-ion imprinted material.

2.4. Synthesis of Copper-ion Imprinted Sensor with VCz

Copper-ion imprinted polymeric resins were synthesized using a molar ratio of 1:1:40 ($Cu(NO_3)_2.2H_2O$: MAA : EGDMA). The prepolymer complex of Copper(II) ion with VCz was prepared by stirring a mixture of 0.1 mmol of copper nitrate and 0.1 mmol of VCz in 5 ml of DMSO for 30 minute. Then the solution was polymerized with the functional monomer (MAA) and cross-linking monomer (EGDMA) using AIBN as initiator. After that the solution was transferred to glass tube with a 4 mm of diameter covered with teflon band. The polymerization was carried out at 60 °C during 24 h after the solution was degassed under vacuum.

2.4.1. Removal of the copper-ion from the synthesized polymers

The copper-ions were leached from the above synthesized polymeric sensor materials by stirring with 100 ml of 50 % (v/v) HCl for 18 h. The resultant resin materials, shape of cylindrical obtained after washing with water were dried in an vacuum desiccater at room temperature to get iron-ion imprinted resin.

2.5 Synthesis of Zinc-ion Imprinted and Nonimprinted Polymers with BCM

The prepolymer complex of Zn^{2+} ion with BCM was prepared by stirring a mixture of 50 mM $Zn(CH_3COO)_2.2H_2O$ and 50 mM BCM in DMSO for 30 min. The prepolymerization mixtures were prepared by adding 100 mM of MAA as a functional and 2M of EGDM as a crosslinking monomer and stirring for further 30 min. Nonimprinted polymer as a control polymer corresponding to same functional and crosslinking monomers were prepared under identical conditions without the addition of Zn^{2+} imprint ion. The prepolymerization mixtures were then transferred to narrowly spaced teflon mould covered with glass plates. After the solution was degassed under vacuum, the polymerization was carried out at 60 °C during 24 h.

2.6 Synthesis of Copper-ion Imprinted and Nonimprinted Polymers with BCM

The prepolymer complex of Cu^{2+} ion with BCM was prepared by stirring a mixture of 50 mM $Cu(NO_3)_2.3H_2O$ and 50 mM BCM in DMSO for 30 min. The prepolymerization mixtures were prepared by adding 100 mM of Vim as a functional and 2M of EGDM as a crosslinking monomer and stirring for further 30 min. Nonimprinted polymer as a control polymer corresponding to same functional and crosslinking monomers were prepared under identical conditions without the addition of Cu^{2+} imprint ion. The prepolymerization mixtures were then transferred into teflon mould with a shape of semi-cylindrical ad covered with glass plates. After the solution was degassed under vacuum, the polymerization was carried out at 60 °C during 24 h.

2.7 FTIR-ATR (Attenuated Total Reflectance-Infrared) Spectroscopy

Attenuated total reflectance (ATR) spectroscopy is a versatile, nondestructive technique for obtaining the infrared spectrum of the surface of a material or the spectrum of materials either too thick or too strongly absorbing to be analyzed by standard transmission spectroscopy.

Structures of imprinted and nonimprinted materials were analysed by FTIR Reflectance Spectrometer (Perkin Elmer with an ATR attachment of spectrum one Universal ATR- with diamond and ZnSe).

2.8 Fluorescence Measurements

Fluorescence spectra were measured by a JASCO FP-750 spectrophotometer (Japan Spectroscopic Co.Ltd.) at 25 ^{0}C; the slits for the excitation and emission monochrometers were 5.0nm and the spectral scan rate was 50.0nm/min. Measurements were made at the 90° position for plate thin dried resin, which has dimension of 0.9 mm x 5 mm x 10 mm, was attached to the sample cell diagonally to make the excited and emitted light is perpendicular to each other. Meanwhile, semi-cylindrical resins were mounted to the surface of the glass plate and cylindrical materials hanged on the center of quartz cell. The reason for producing cylindrical shaped material was to minimize the reflection of light coming from surface of plate materials attached to the cell diagonally.

3.RESULTS AND DISCUSSION

3.1 Interaction of VCz with Metal Ion

The interactions of metal ions with VCz were investigated by spectrofluorometric method. Figure 3.1 shows the change of excitation spectra of VCz in acetonitrile upon titration with Cu^{2+} ion. As seen from Fig. 1, VCz exhibits two excitation maximum wavelengths at 282 nm and 342 nm, which shift to 276 and 344 nm upon binding to copper (II) metal ion. Meanwhile, decrease in excitation intensity of VCz is observed depending on complex formation with Cu(II) metal ion.

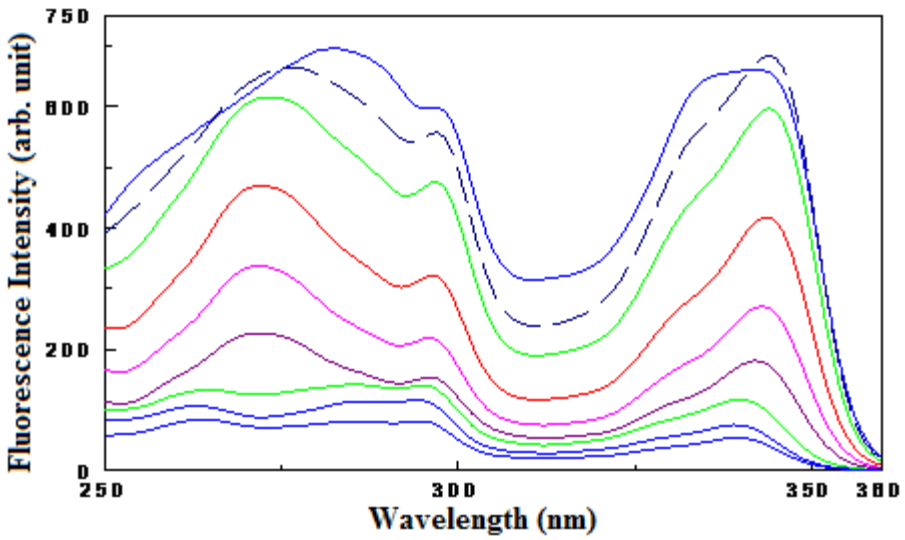

Figure 3.1: Excitation spectra of $4x10^{-5}$ M VCz in acetonitrile in the presence of different concentration of Cu^{2+}.($\lambda_{em} = 367$).

When excited at 332 nm, VCz shows an emission maximum at 367 nm, which does not shift upon binding of Cu(II) metal ion (Figure 3.2). From this figure, it is evident that fluorescence emission intensity of VCz decreases dramatically depending on complex formation with Cu(II) metal ion. This decrease of emission intensities may

be due to the formation of coordination complex of N-atom on VCz with Cu(II) metal ion.

These coordination complex makes the energy transfer from the excited state of VCz to Cu(II) metal ion possible, thus increase the non-radiated transition of VCz excited state and decrease the fluorescence emission.

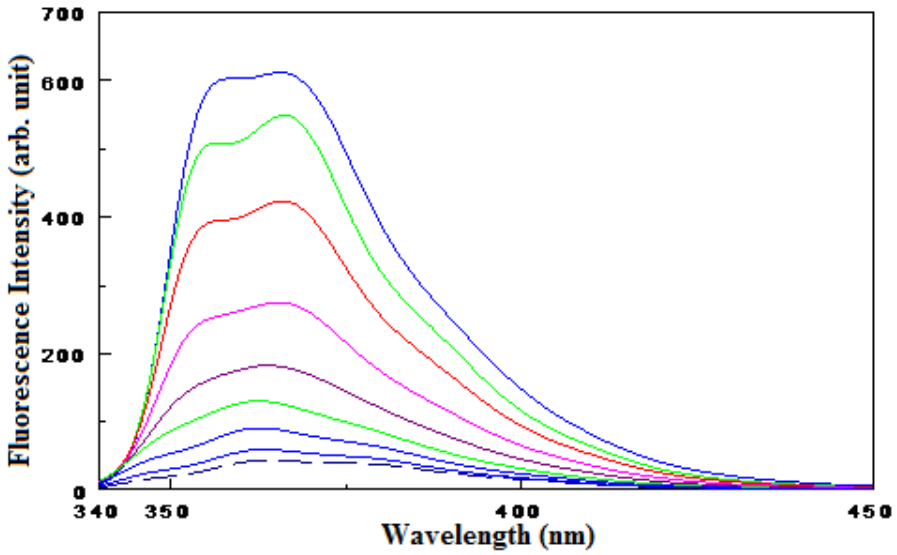

Figure 3.2: Emission spectra of $4x10^{-5}$ M VCz in acetonitrile depending on Cu^{2+} concentration ($\lambda_{ex} = 332$).

The efficiency of quenching a fluorescent VCz by a quenching metal ion can be described by the Stern–Volmer relationship, if the fluorophore and the quencher concentrations are within the appropriate range:

$$\frac{F_0}{F} = 1 + K_{SV}[Q] = 1 + k_q \tau_0 [Q]$$

where F_0 is the fluorescent intensity in the absence of a metal ion, F is the fluorescent intensity in the presence of a metal ion at concentration [Q], kq is the quenching rate constant, τ_0 is the lifetime of the excited state in the absence of a metal ion, and Ksv is the Stern–Volmer constant. If a system follows the Stern–Volmer equation, a plot of F_0 / F versus [Q] will give a straight line with a constant slope of Ksv and an intercept of 1 at the y-axis. Ksv is therefore a measure of quenching efficiency.

Figure 3.3 shows the changing of fluorescence emission intensity of VCz at 367 nm depending on Cu(II) metal ion concentration. Emission intensity of VCz is decreased when metal ion concentration is increased. As seen from figure, Stern–Volmer plot does not show linearity. Deviation of the plot of F_0 / F against [Q] from linearity also indicates that static and dynamic quenching may occur simultaneously.

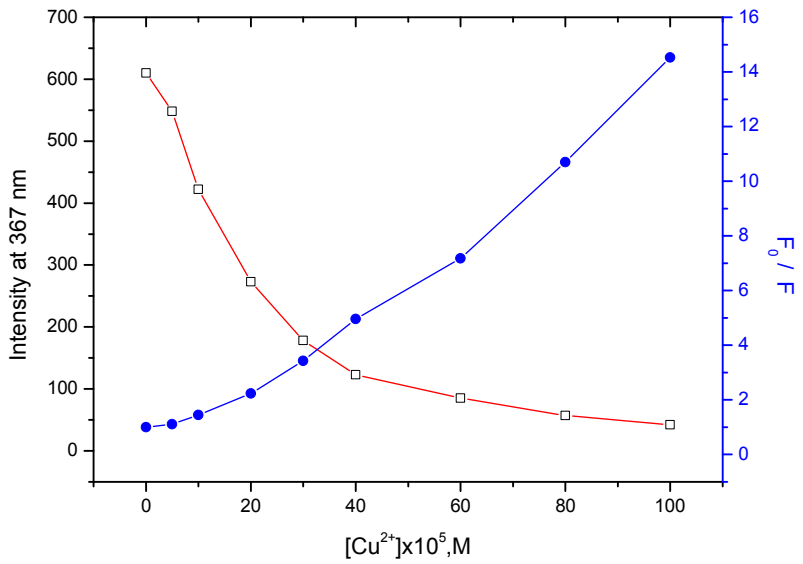

Figure 3.3: Stern-Volmer plot of emission of $4x10^{-5}$ M VCz in acetonitrile quenched by Cu^{2+} ion. ($\lambda_{ex} = 332$).

3.1.1 FTIR-ATR spectra of Pb-imp and nonimp polymers

Surfaces of imprinted and nonimprinted sensor materials were analyzed by FTIR-ATR Reflectance Spectrometer to elucidate the weather imprinted material is identical with nonimprinted material after lead ion was removed from sensor. Figure3.4 demonstrates FTIR-ATR spectra of sensor materials prepared at the same reaction conditions in the absence and the presence of lead ion. Vibrational modes of each peak in two spectra can be given in details. Peaks at 2951cm^{-1} and 2928 cm^{-1} are characteristics of the stretching vibration of aliphatic C-H groups. Peaks at 1722 cm^{-1} and 1716 cm^{-1} are attributable to the stretching vibration of carbonyl groups of

ester structure. Bands in 1453 cm^{-1} and 1387 cm^{-1} originate from C-H bandings and plane bendings.

The bands at approximately 1244 cm^{-1} and 1141 cm^{-1} are assigned to the symmetric and asymmetric stretching modes of the C-O-C bonds in ester groups. The result of FTIR-ATR analysis reveals that template lead (II) metal ion was completely removed from sensor material by washing procedure, showing the identical structure of imprinted and nonimprinted materials.

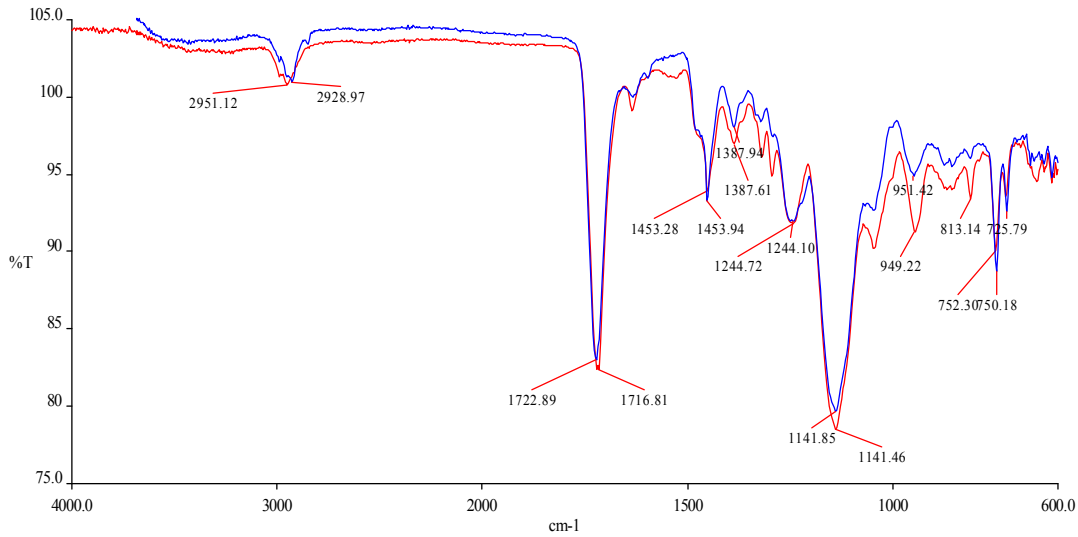

Figure 3.4: FTIR-ATR spectra of Pb-imp and nonimp polymers.

3.1.2 Pb^{2+} binding capability of Pb-imprinted and nonimprint materials

Figure 3.5 shows the emission spectra of Pb-imprinted plane sensor in the presence of different concentration of lead ion in aqueous solution. It was observed that fluorescence emission of sensor was decreased as the concentration of lead ion in aqueous solution was increased. Quenching of emission may be based on the heavy atom effect which causes to the changing of singlet excited state to the triplet excited state resulted in radiationless emission.

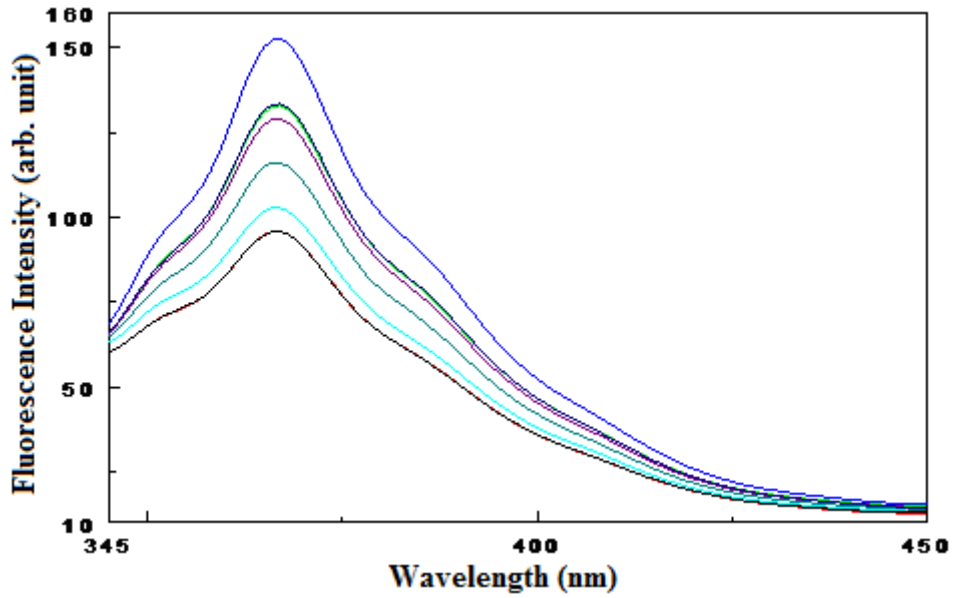

Figure 3.5: Effects of Pb^{2+} concentrations on the fluorescence spectra of Pb-imp sensor containing PVCz. (λ_{ex} = 332 nm).

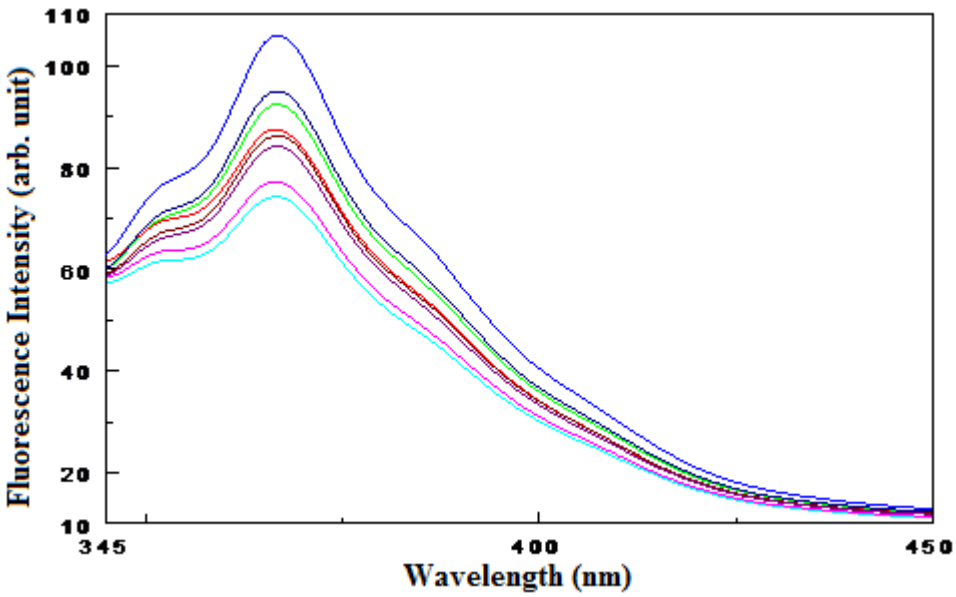

Figure 3.6: Emission spectra of nonimp polymer containing PVCz depending on Pb^{2+} concentrations(λ_{ex} = 332 nm).

In case of nonimprinted material which was synthesized in the absence of metal ion, also quenching of emission intensity of VCz in sensor was observed depending on lead (II) metal ion in aqueous solution (Figure 3.6).

The increase in quenching effect may show the metal ion binding ability of sensor. Figure 3.7 exhibits the decrease of emission intensity of each imprint and nonimprint sensors upon increase of lead metal ion concentration in aqueous solution. As seen from figure, emission intensity of VCz in imprinted sensor is more quenched that that of VCz in nonimprinted sensor at the range of 10^{-4} and 10^{-3} M. There is no remarkable difference in quenching of emission at lower concentration of lead ion than 10^{-4} M.

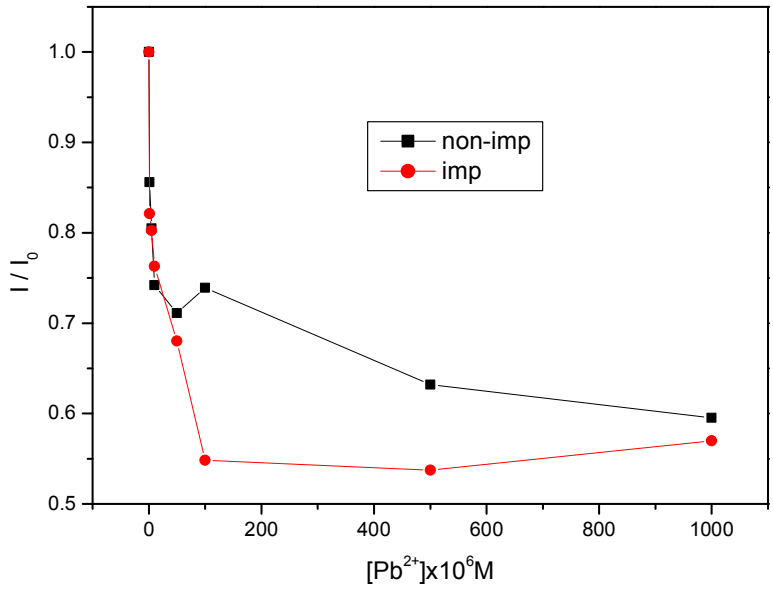

Figure 3.7: Pb^{2+} dependence of emission intensity of Pb-imp and nonimp polymers containing PVCz. (λ_{ex} = 332 nm).

Lead ion adsorption experiment were carried out in 0.1 M $NaNO_3$ containing aqueous solutions to differentiate the lead ion binding properties of each sensor since electrolyte in solution reduces the one hand binding of methacrylic acid to the lead (II) metal ion.

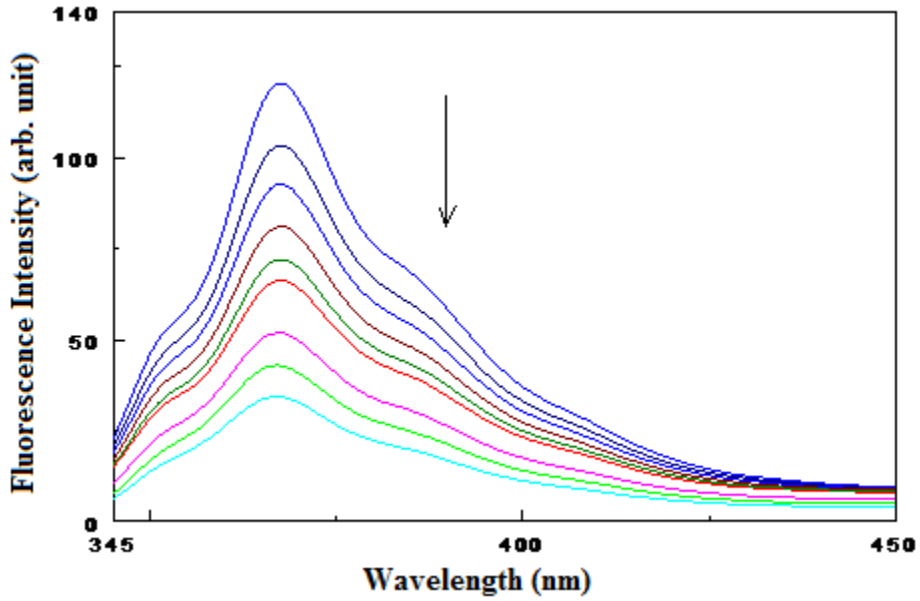

Figure 3.8. Fluorescence emission spectra of Pb-imp sensor in the presence of different concentration of Pb^{2+} ion in aqueous solution containing 0.1 M $NaNO_3$. Arrow shows the increase in Pb^{2+} ion concentration.

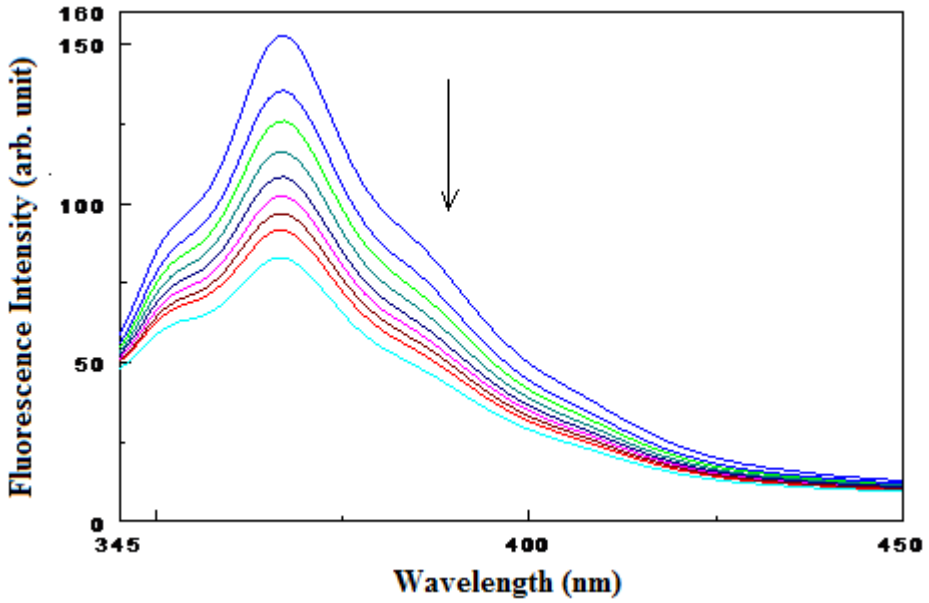

Figure 3.9: Fluorescence spectra of nonimp polymer in the presence of different concentration of Pb^{2+} ion in aqueous solution containing 0.1 M $NaNO_3$. Arrow shows the increase in Pb^{2+} ion concentration.

Figure 3.8 and 3.9 show the emission spectra of imp and nonimprinted metarial upon interaction with increasing lead metal ion concentration prepared in the presence of 0.1 M $NaNO_3$. As seen from figures, emission intensity of each sensor is quenched by lead ion. The binding affinity or interaction capability of each sensor can be distinguished when the decrease in emission intensity is plotted as a function of lead ion concentration (Figure 3.10). It is clear from figure that emission intensity of VCz in imprinted sensor is more quenched than that of VCz in nonimprinted material. This indicates that imprinted sensor has more metal ion-binding sites than that of nonimprinted, and also shows the memory of pairing of methacrylic acids within the sensor.

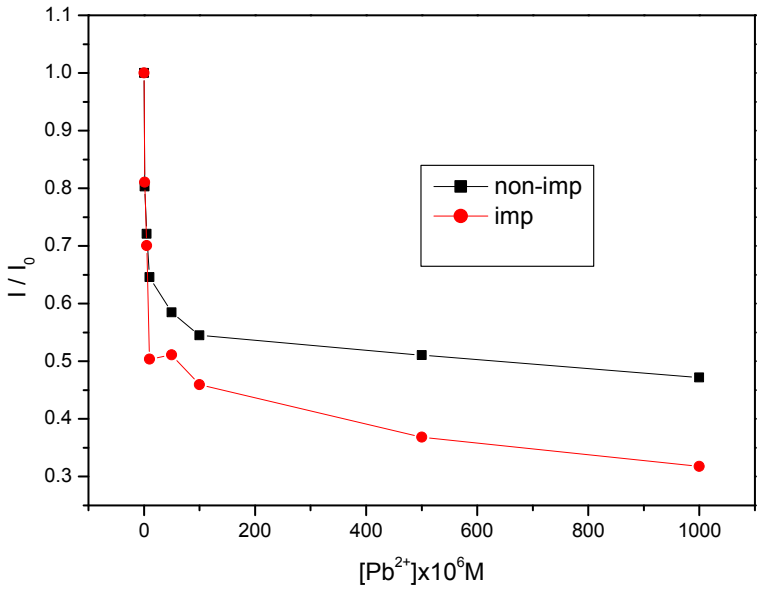

Figure 3.10 : Dependence of emission intensity of Pb-imp and nonimp polymers containing PVCz to the Pb^{2+} concentration in 0.1 M $NaNO_3$ ($\lambda_{ex} = 332$ nm).

Responses of lead ion imprinted and randomly synthesized sensor (nonimprinted) to Hg(II) metal ion were tested using single concentration of Hg(II) ion as a function of time. (figure 3.11). Decrease in emission intensity is more pronounced in the case of imprinted sensor showing the more binding sites on the surface of the imprinted material.

On the other hand, quenching of emission intensity of lead-ion imprinted sensor in the presence of Hg(II) ion indicates that cavity formed on sensor has low selectivity.

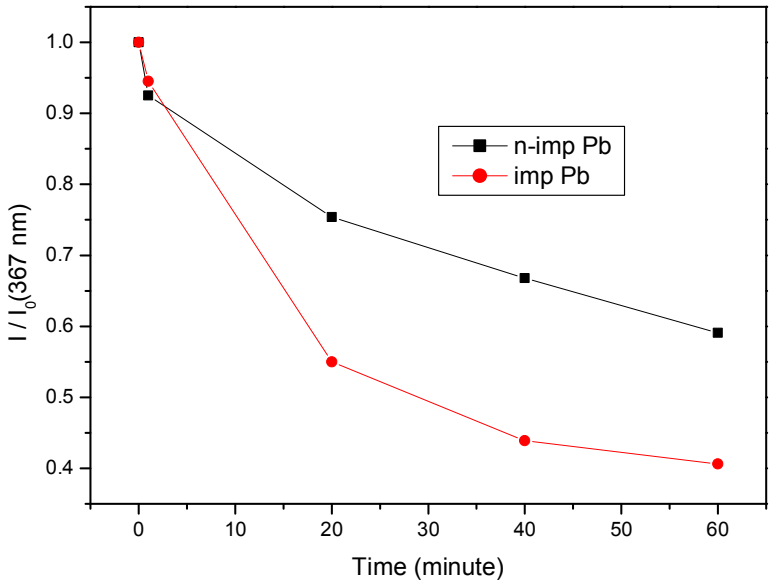

Figure 3.11: Plot of I / I_0 for Pb-imp and nonimp polymers as a function of time obtained in the presence of $5x10^{-4}$ M Hg^{2+} in aqueous solution. ($\lambda_{ex} = 332$ nm).

3.1.3. Comparison of Fe^{2+} affinities of Fe-imprinted and nonimprinted polymers

Figure 3.12 shows the emission spectra of iron-ion imprinted cylindrical sensor depending on different concentrations of iron ion in aqueous solution. As seen from figure, fluorescence emission of imprinted sensor was decreased as the concentration of Fe^{2+} in aqueous solution was increased. The reason of decrease of emission may be due to either heavy atom effect which causes to the changing of singlet excited state to the triplet excited state resulted in radiationless emission or inner filter effect caused by overlapping of excited wavelength of VCz with absorption spectra of iron ion salt which is colourful in natural form.

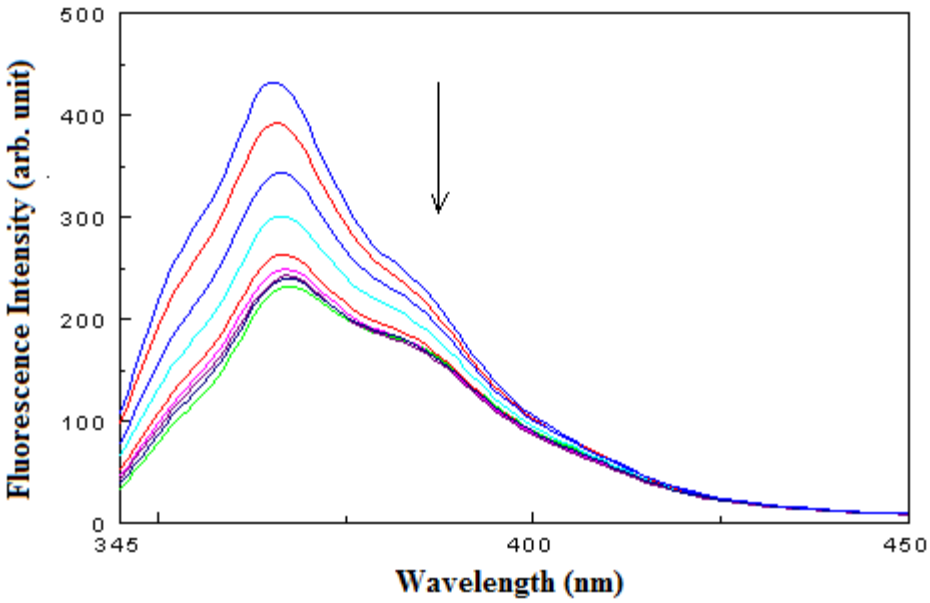

Figure 3.12: Emission spectra of Fe-imp sensor containing PVCz upon Fe^{2+} concentrations in aqueous solution. ($\lambda_{ex} = 332$ nm)

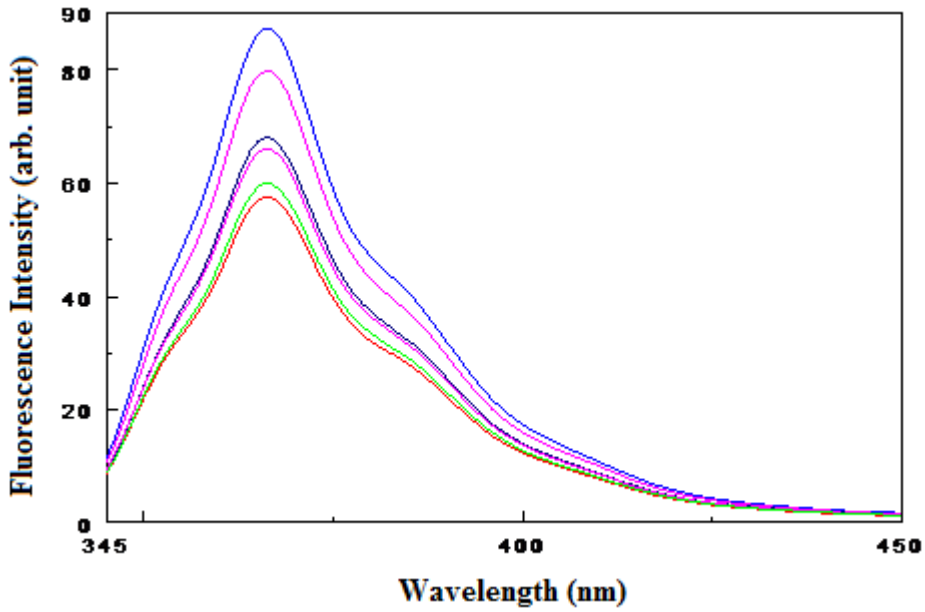

Figure 3.13: Dependence of emission spectra of nonimp polymer containing PVCz in the presence of Fe^{2+} concentrations in aqueous solution. ($\lambda_{ex} = 332$ nm)

Nonimprinted material which was synthesized in the absence of Fe^{2+} ion also exhibits emission changing upon interaction with iron(II) ion in aqueous solution.(figure 3.13). This indicates that randomly polymerized material containing VCz give response the iron ion showing the sensor property. On the other hand, imprinted sensor exhibits higher affinity than nonimprinted material as comparing the quenching of emission of VCz in polymer matrix (figure 3.14).

The difference in quenching of emission implies the formation of cavity in imprinted sensor which provides more binding sites for adsorption of iron metal ions.

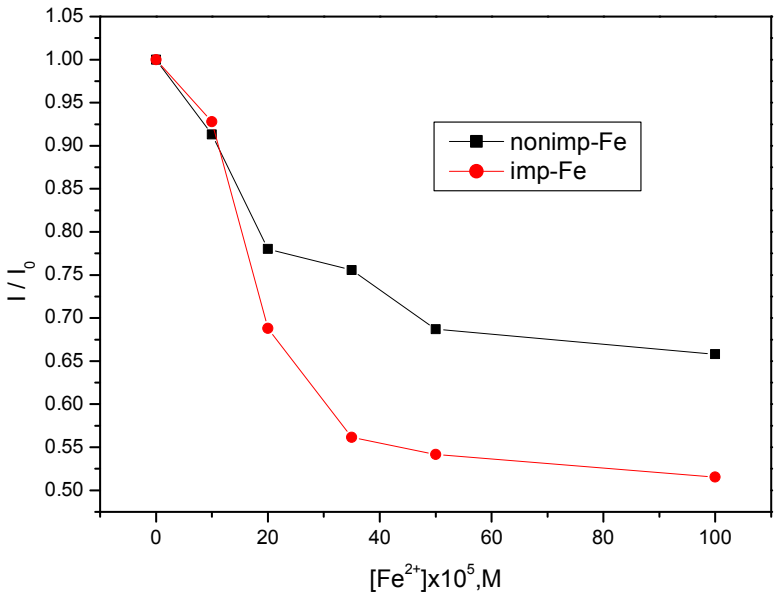

Figure 3.14: Changing of emission intensity of Fe-imp and nonimp polymers containing PVCz depending on Fe^{2+} concentrations. Emission spectra were obtained after waited 30 minute in the presence of Fe^{2+} metal ions. ($\lambda_{ex} = 332$ nm)

3.1.4. Affinities of Cu-imprinted and nonimprinted materials to Cu^{2+}

Emission spectra of copper-ion imprinted sensor which has cylindrical shape were monitored depending on different concentrations of copper ion in aqueous solution.(Figure 3.15). Fluorescence emission of imprinted sensor increase as the concentration of Cu^{2+} in aqueous solution was increased.

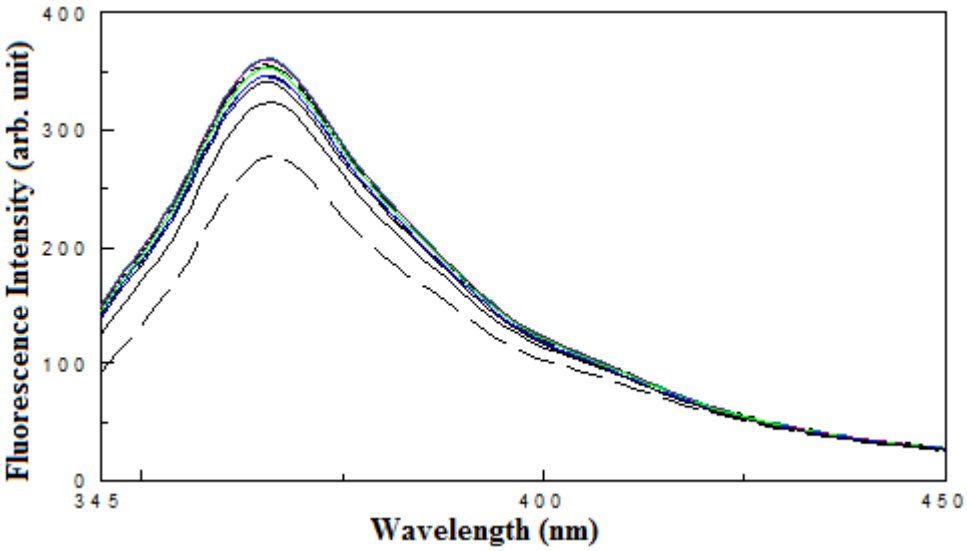

Figure 3.15: Fluorescence emission spectra of Cu-imp sensor containing PVCz depending on Cu^{2+} concentrations. ($\lambda_{ex} = 332$ nm).

Figure 3.16 shows the emission spectra of nonimprinted cylindrical material which was prepared without using copper ion in polymerization solution. Increase in emission intensity of VCz in nonimprinted material was not pronounced depending on concentrations of cooper ion. Plot of I / Io against copper ion is obtained using the maximum emission intensities of VCz in sensor material for each copper ion concentration.(Figure 3.17). From figure it can be seen that increase in emission intensity of imprinted material upon interaction with copper ion is more than that of nonimprinted material.

On the contrary to the behavour of other lead-ion and iron-ion imprinted nonimprinted materials, increases in emission intensity of VCz in copper-ion imprinted and nonimprinted sensors were unclear at present.

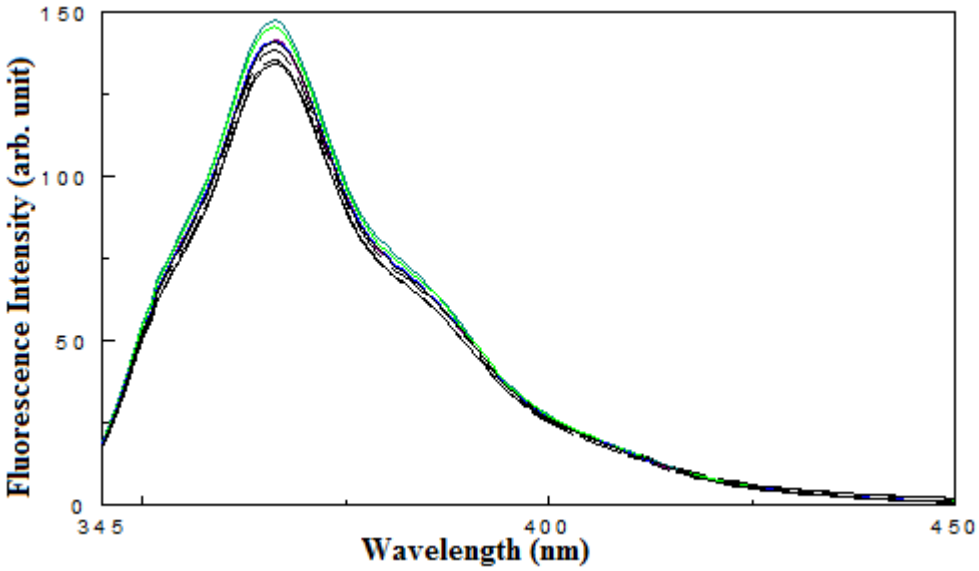

Figure 3.16: Emission spectra of nonimp polymer in the presence of Cu^{2+} concentrations. Emission spectra were obtained after waited 30 minute in the presence of metal ions.

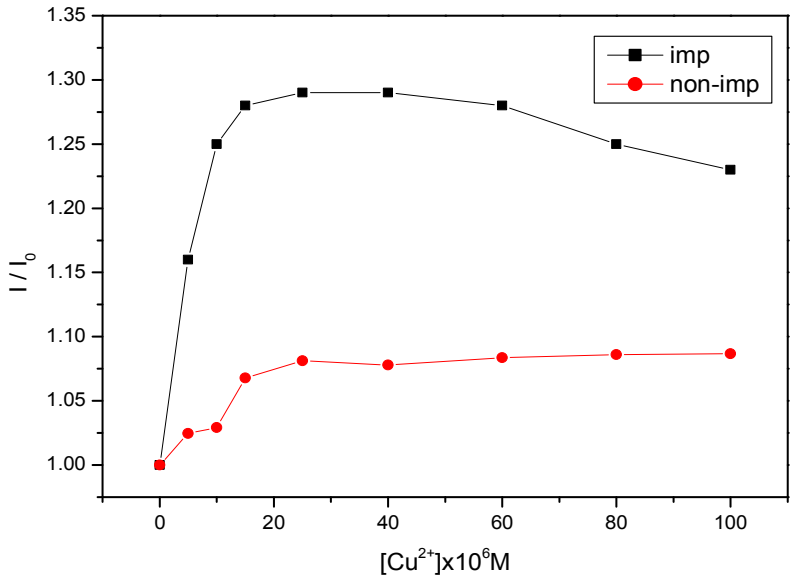

Figure 3.17: Changing of I / I_0 values at 367 nm of Cu-imp and nonimp polymers versus Cu^{2+} concentrations. ($\lambda_{ex} = 332$ nm).

3.2. Photophysical Properties of BCM

Fluorescence excitation and emission spectra of BCM monomer were obtained depending on different concentrations in DMSO solution since this monomer was newly synthesized (Figure 3.18). Spectral analysis reveals that BCM shows maximum excitation wavelength at 385 nm at low concentrations. As the concentration is increased, excitation intensity increased and maximum excitation wavelength shifts to red region. On the other hand, excitation intensity begins to decrease from the higher concentration than 10^{-4} M. This decrease in emission intensity at high concentration of substance in solution is attributed to the selfquenching of emission. BCM monomer exhibits maximum emission wavelength at 510 nm when samples of BCM in solvent with different concentrations are excited at 410 nm.(figure 3.18, right spectra). There is any spectral shift in maximum wavelength upon increasing of BCM concentrations. Same behavior of emission intensity was observed at high monomer concentration in solution like excitation spectra (figure 3.19).

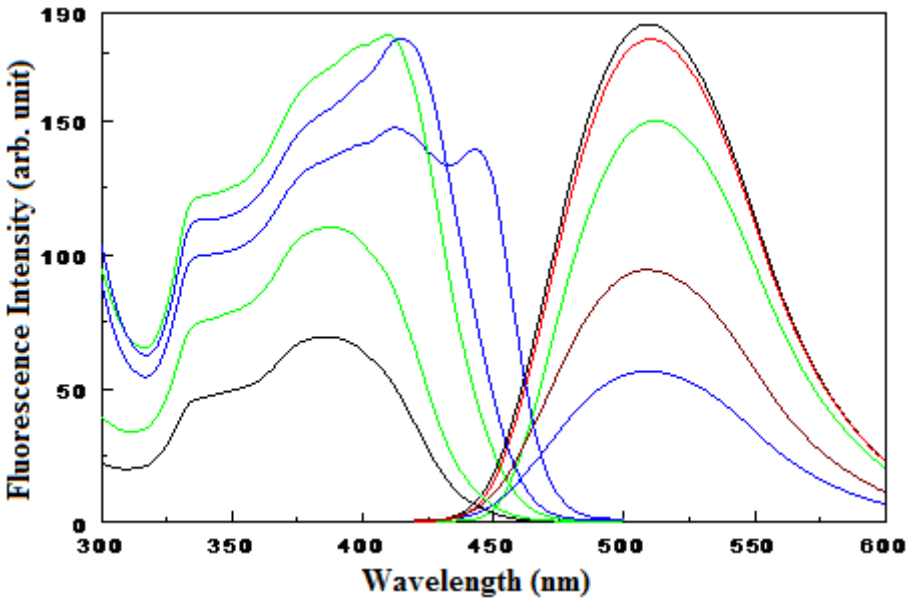

Figure 3.18: Excitation and emission spectra of BCM in DMSO depending on concentration . ($\lambda_{ex} = 410$ nm and $\lambda_{em} = 510$ nm)

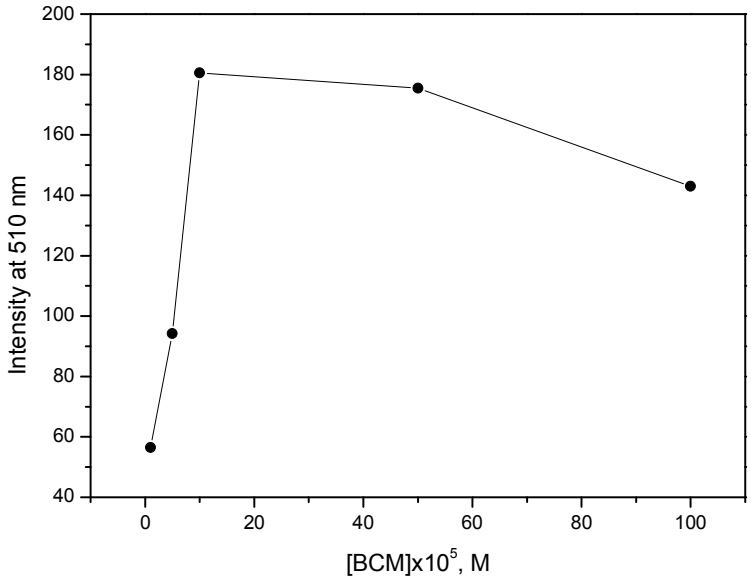

Figure 3.19: Emission intensities of BCM in DMSO depending on concentration. $\lambda_{ex} = 410$ nm

3.2.1 Titration of BCM with metal ion

Fluorescence titration was carried out to elucidate the affinity of metal ion binding of BCM in different solvents which have different dipol moment and dielectric constant. Figure 3.20 shows the fluorescence spectra of BCM depending on addition of copper ion in DMSO. Emission intensity of BCM is quenched in the presence of Cu^{2+}. The emission intensity at 510 nm depending on Cu^{2+} concentration was plotted (figure 3.21). It is seen from figure, as the cooper concentration is increased, the emission intensity of BCM is decreased showing that the interaction of BCM with copper ion.

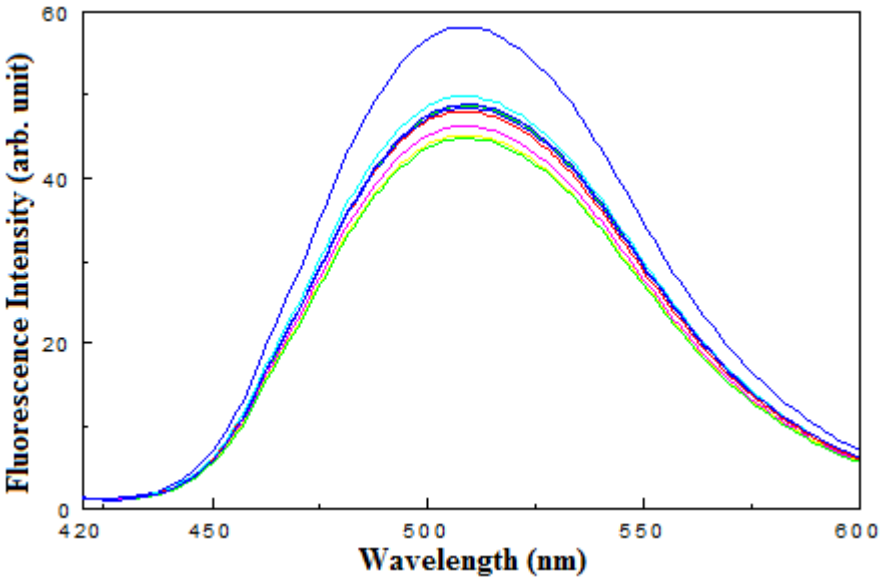

Figure 3.20: Fluorescence spectra of $2x10^{-5}$ M BCM in DMSO depending on Cu^{2+}. ($\lambda_{ex} = 410$ nm)

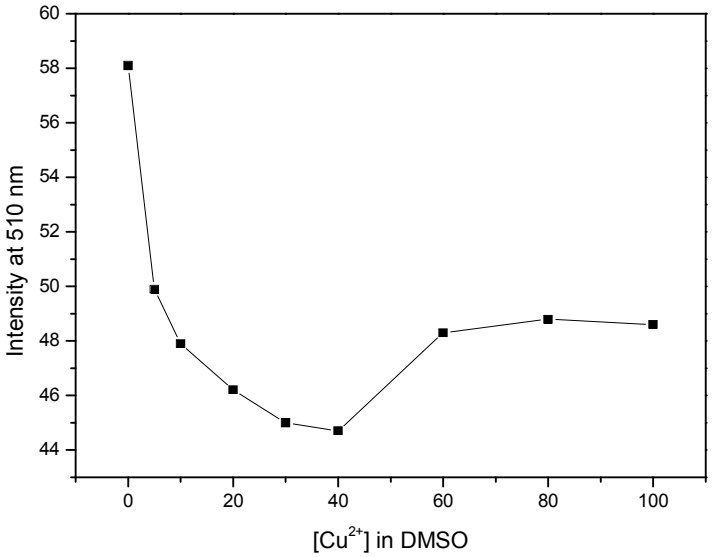

Figure 3.21: Cu^{2+} dependence of emission intensity at 510 nm of $2x10^{-5}$ M BCM in DMSO. ($\lambda_{ex} = 410$ nm).

Figure 3.22 and 3.23 show the emission spectra of $2x10^{-5}$ M and $2x10^{-4}$ M BCM in ethanol upon addition of mercury ion in ethanol. In both cases, quenching of emission by Hg^{2+} ion was observed. But quenching of emission depending on Hg^{2+} ion is more pronounced in low concentration of BCM.

This observation is important for developing sensitive sensor material using floroprope molecules embedded in polymer matrix.

And as seen from figure 3.24, the fluorescence response of BCM to mercury ion is very depended on concentration. Fluorescence signal reduces causing to low sensitivity at high concentrations .

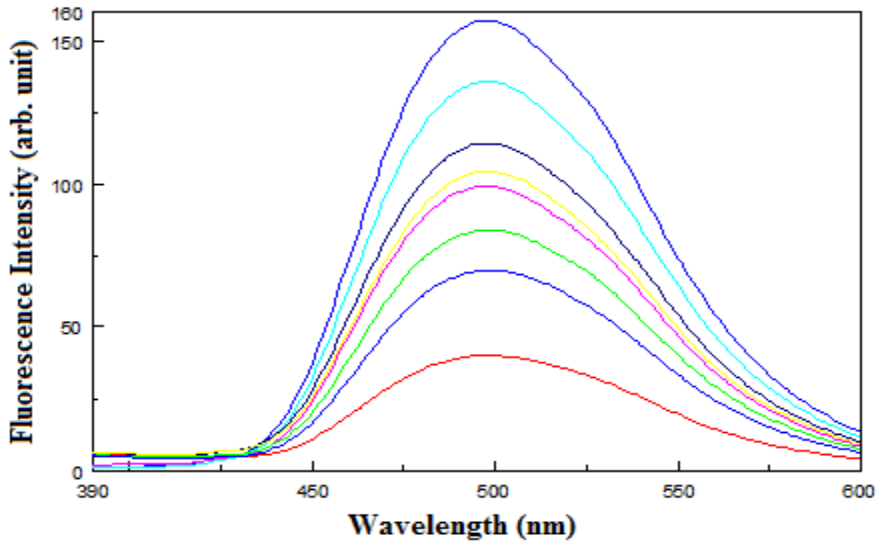

Figure 3.22: Emission spectra of $2x10^{-5}$ M BCM in ethanol in the presence of Hg^{2+}. ($\lambda_{ex} = 410$ nm).

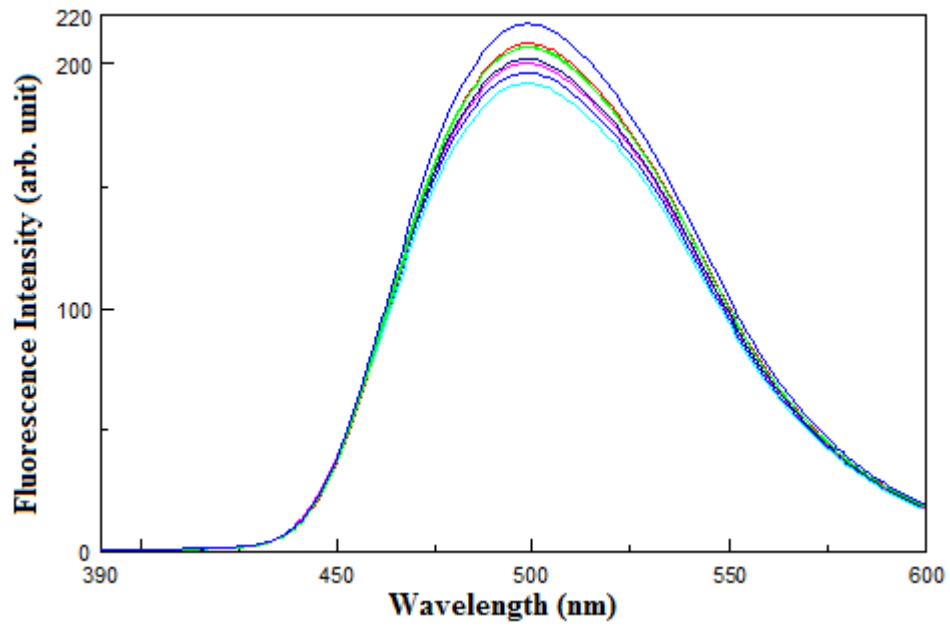

Figure 3.23: Emission spectra of $2x10^{-4}$ M BCM in ethanol depending on titration with Hg^{2+}.($\lambda_{ex} = 410$ nm).

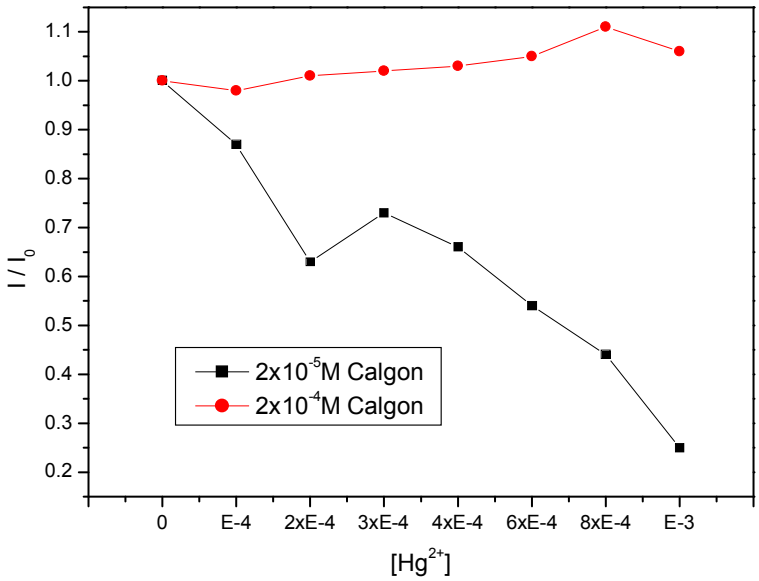

Figure 3.24: Dependence of emission intensities of BCM at different concentrations to Hg^{2+}.($\lambda_{ex} = 410$ nm).

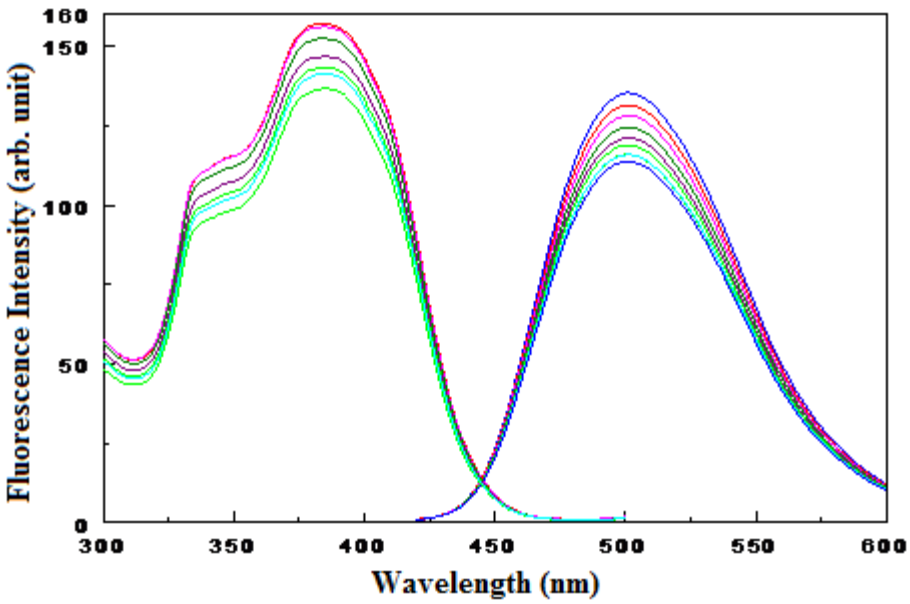

Figure 3.25: Excitation and Emission spectra of $2x10^{-5}$ M BCM in 2-Methoxy ethanol depending on titration with Hg^{2+}. ($\lambda_{ex} = 410$ nm and $\lambda_{em} = 500$ nm)

Fluorescence titration of BCM with Hg^{2+} ion was carried out using the 2-Methoxy ethanol as a solvent.(figure 3.25). Figure shows the excitation and emission spectra of BCM in 2-Methoxy ethanol depending on Hg^{2+} ion concentration.

Both intensity of excitation and emission spectra are decreased as Hg^{2+} is added to the solution containing BCM. On th other hand, same fluorescence behavior of BCM in acetonitrile was observed in the presence of mercury ion.(Figure 3.26) Figure shows the excitation and emission spectra of BCM in acetonitrile depending on Hg^{2+} ion concentration. Both intensities of excitation and emission spectra are decreased as Hg^{2+} is added to the solution. Figure 3.27 shows the decrease of emission intensity of BCM in 2-Methoxy ethanol and acetonitrile upon Hg^{2+} ion addition. As seen, same quenching effect was observed when compared the titrations in each solvent.

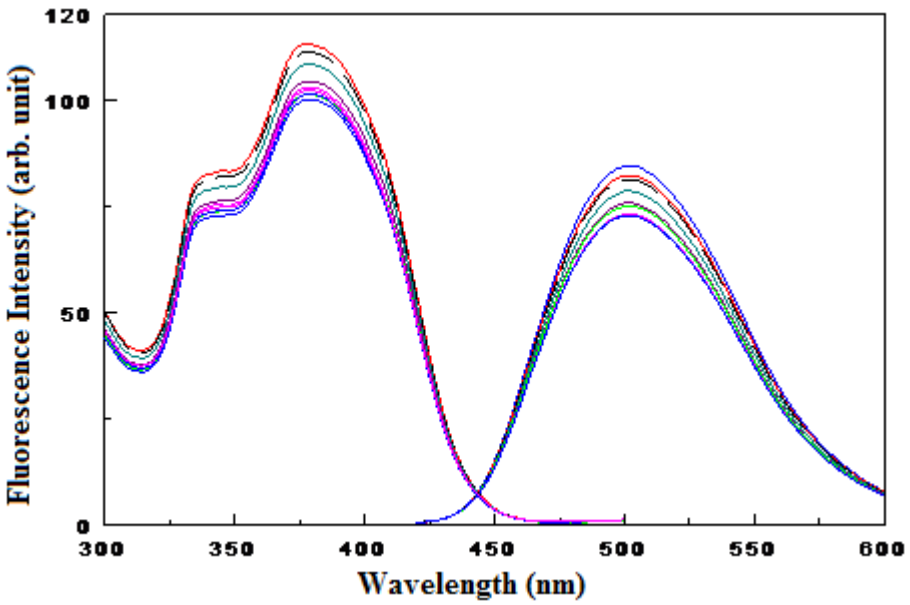

Figure 3.26: Excitation and Emission spectra of $2x10^{-5}$ M BCM in acetonitrile depending on titration with Hg^{2+}. ($\lambda_{ex} = 410$ nm and $\lambda_{em} = 500$ nm)

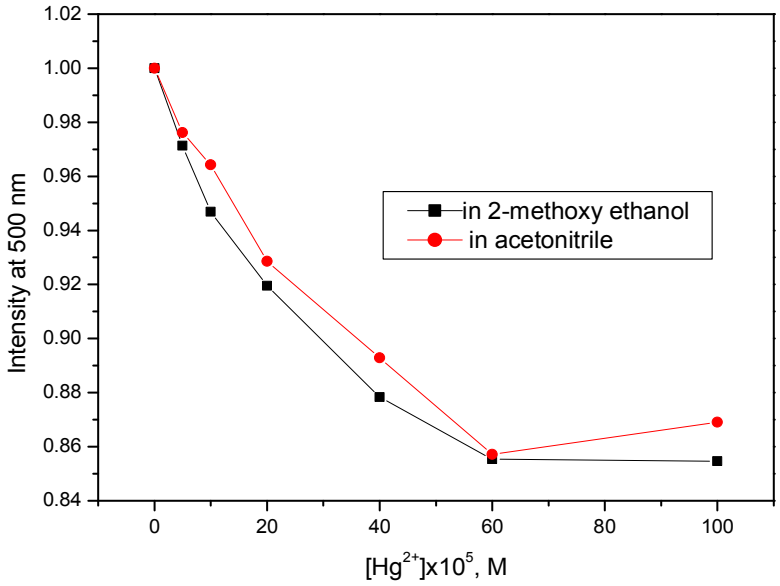

Figure 3.27: Hg^{2+} dependence of emission intensity of $2x10^{-5}$ M BCM in different solvents.

3.2.2. FTIR-ATR Spectra of Zn-imp and Nonimp Polymers

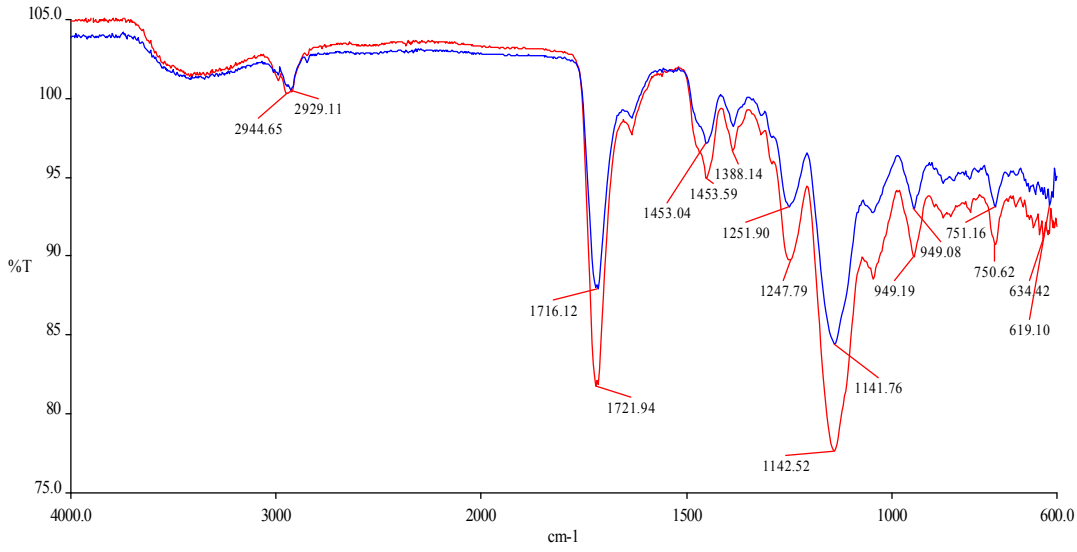

Figure 3.28: FTIR-ATR spectra of Zn-imp and nonimp polymers containing BCM.

The FTIR-ATR spectra of zinc-ion imprinted and nonimprinted plate sensor containing BCM were obtained from the surface of the materials reflectance measurements (figure 3.28).

Spectra show that the both of two have identical chemical structure after zinc ion was removed from imprinted sensor. Vibrational modes in two spectra were almost same with that of polymeric materials containing VCz. This indicates that vibratioanal modes of EDMA are dominant compared to that of BCM and VCz because of the relative concentration ratio.

3.2.3 Fluorescence spectra of Zn-imprinted and nonimprinted polymers containing BCM against to pH

The pH dependence of the emission spectra is shown in Figure 3.29. The experiment of the effect of pH on imprinted sensor was carried out at a pH range from 7 to 11. It can be seen that, the fluorescence intensity of the sensor decreased with increasing pH value. The evolution of the fluorescence spectra of nonimprinted material versus pH was similar to that of the imprinted sensor (Figure 3.30). In other words, when increasing the pH, emission bands of the nonimp resin also are decreased.

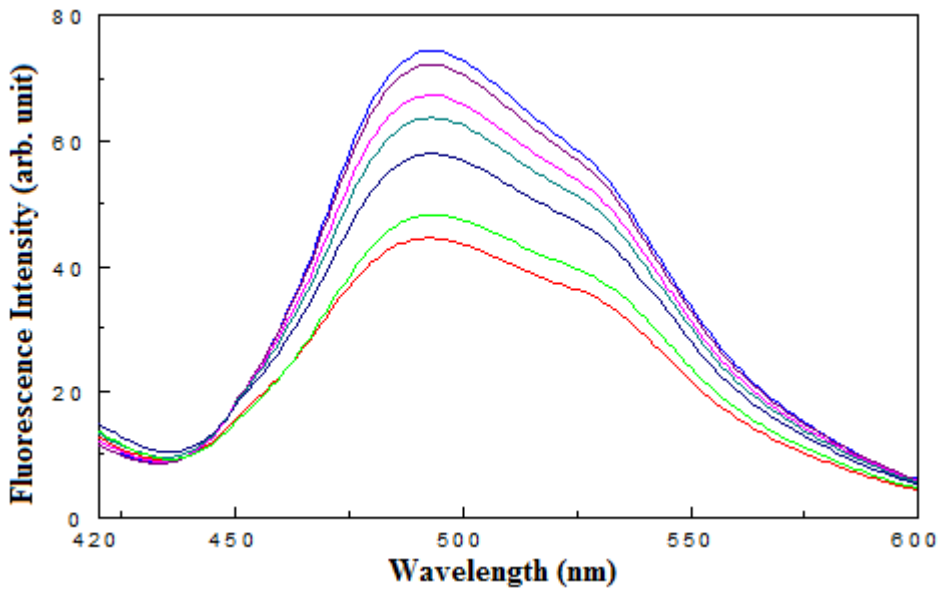

Figure 3.29: Fluorescence response of Zn-imp plane sensor containing BCM against to pH in base solution. ($\lambda_{ex} = 410$ nm)

The fluorescence intensity versus pH plot for the imprinted and nonimprinted materials containing BCM shown in Figure 3.31 was obtained by adjusting the solution pH with sodium hydroxide. Fluorescence emission intensity of each sensor is decreased upon increasing values of pH. There is slight difference in pH response of two sensors.

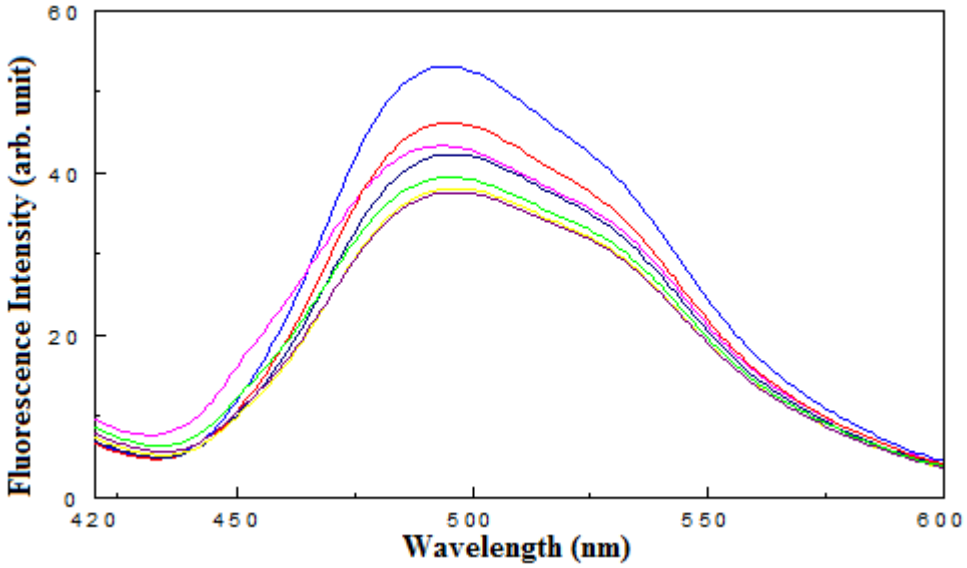

Figure 3.30: pH dependence of fluorescence spectra of nonimp polymer containing BCM in base solution. ($\lambda_{ex} = 410$ nm)

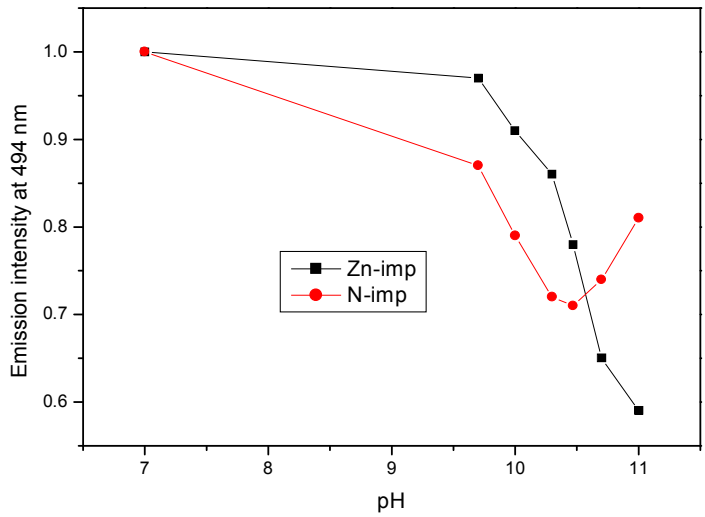

Figure 3.31: Fluorescence emission intensities of Zn-imp and nonimp polymers containing BCM against to pH. ($\lambda_{ex} = 410$ nm)

The fluorescence spectra upon pH values for the zinc ion imprinted sensor shown in Figure 3.32 were obtained by adjusting the solution pH with hydrochloric acid. The experiment of the effect of pH on imprinted sensor was carried out at a pH range from 3 to 7. It can be seen that, the fluorescence intensity of the sensor decreased with decreasing pH value. The effect of pH on nonimprinted sensor was similar to that obtained with imprinted sensor (figure 3.33). Changing of fluorescence intensity depending on pH values was plotted for each sensor (Figure 3.34). Fluorescence emission intensity of each sensor is decreased upon decreasing values of pH. The decrease in emission intensity of imprinted sensor was higher than that of the nonimprinted material.

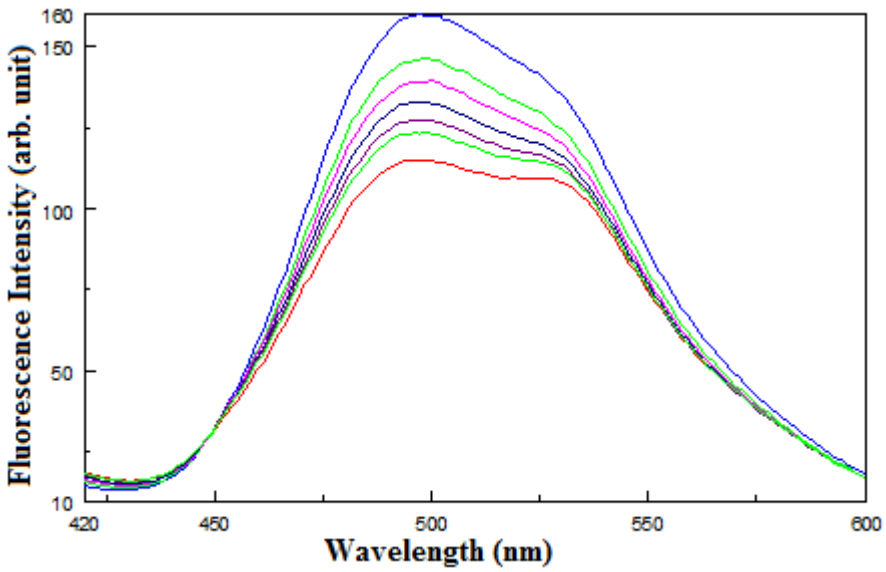

Figure 3.32: Fluorescence response of Zn-imp plate sensor containing BCM against to pH in acid solution. ($\lambda_{ex} = 410$ nm)

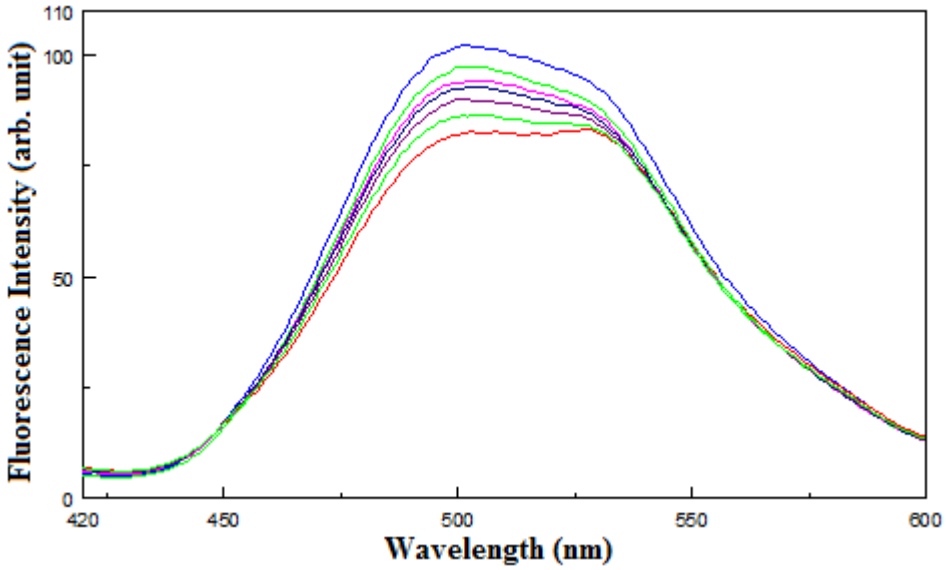

Figure 3.33: pH dependence of fluorescence spectra of nonimp polymer containing BCM in acid solution. ($\lambda_{ex} = 410$ nm)

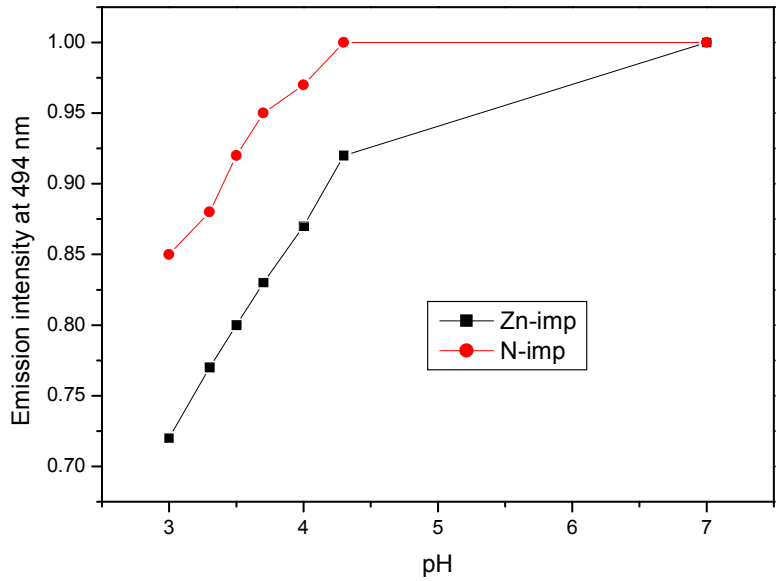

Figure 3.34: Fluorescence response of Zn-imp and nonimp polymers against to pH

3.2.4 Fluorescence response of cylindrical Zn-imprinted and nonimprinted polymers containing BMC to Hg^{2+}

The aim of the synthesis of zinc imprinted sensor containing BCM was to explore the sensitivity and selectivity of BCM towards biologically important metal cations.

On the other hand, the coordination of Zn^{2+} does not give visible changes of fluorescence emission. Therefore the coordination of Hg^{2+} which is paramagnetic transition-metal cation, was investigated using zinc imprinted polymer containing BCM.

The mercury ion effect on emission spectra of Zn-ion imprinted polymer is shown in figure 3.35. As seen from figure, Hg^{2+} ion is quenched the emission of BCM in imprinted sensor. The reason for this phenomenon might be due to collosional quenching or statical quenching which indicates the coordination of Hg^{2+} ion to nitrogen atom on BCM molecule in imprinted material.

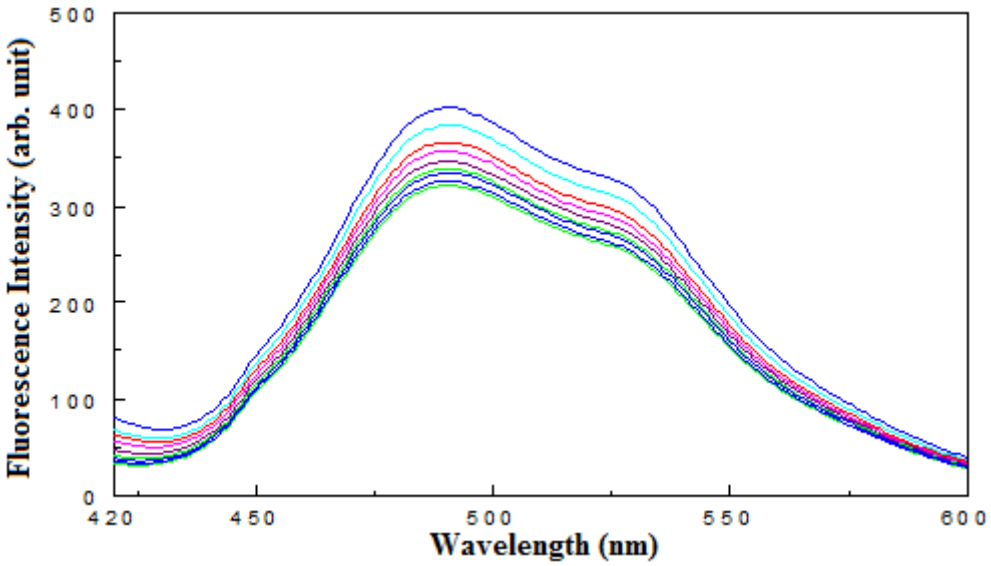

Figure 3.35: Fluorescence Emission spectra of cylindrical Zn-imp sensor containing BCM depending on Hg^{2+} concentrations. ($\lambda_{ex} = 410$ nm)

Figure 3.36 shows the Hg^{2+} metal ion dependence of fluorescence spectrum of nonimprinted material. Hg^{2+} also causes to the quenching of emission of nonimprnted material. Comparison of emission quenching effect was made by plotting I/Io versus Hg^{2+} ion concentration (figure3.37). Emission intensity in imprinted sensor is reduced higher than that of nonimprint material exhibiting the more binding or interacting sides in imprinted material.

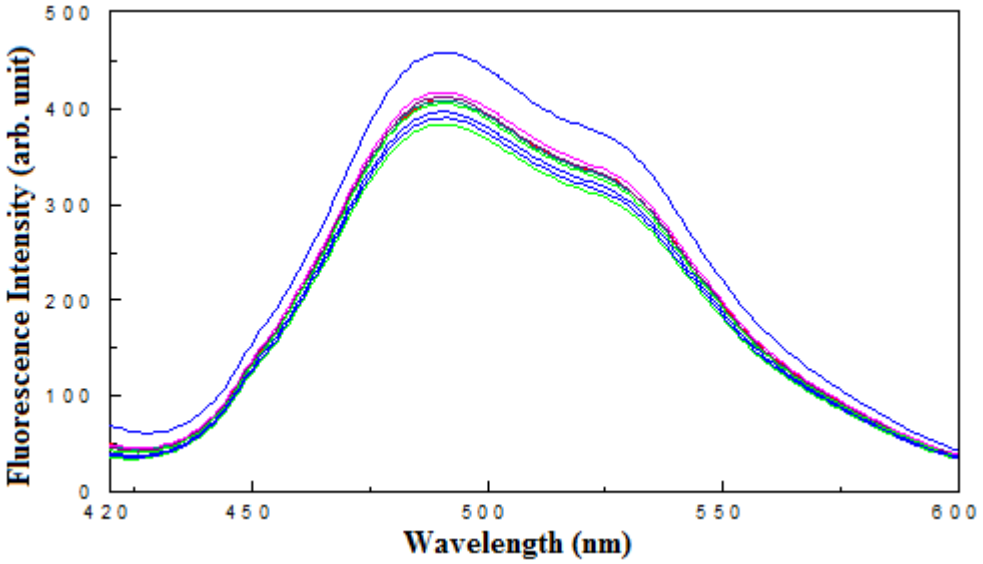

Figure 3.36 : Emission spectra of cylindrical nonimp polymer containing BCM upon titration with Hg^{2+} ion concentration in aqueous solution($\lambda_{ex} = 410$ nm)

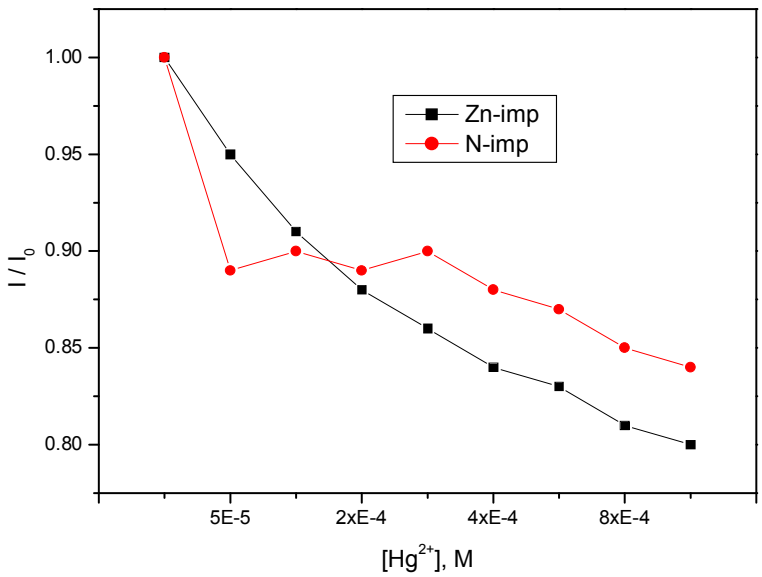

Figure 3.37: Emission intensities of cylindrical Zn-imp and nonimp polymers containing BCM in the presence of Hg^{2+} concentrations. ($\lambda_{ex} = 410$ nm)

3.2.5. Affinities of semi-cylindrical Cu-imprinted and nonimprinted polymers containing BCM to Cu^{2+}

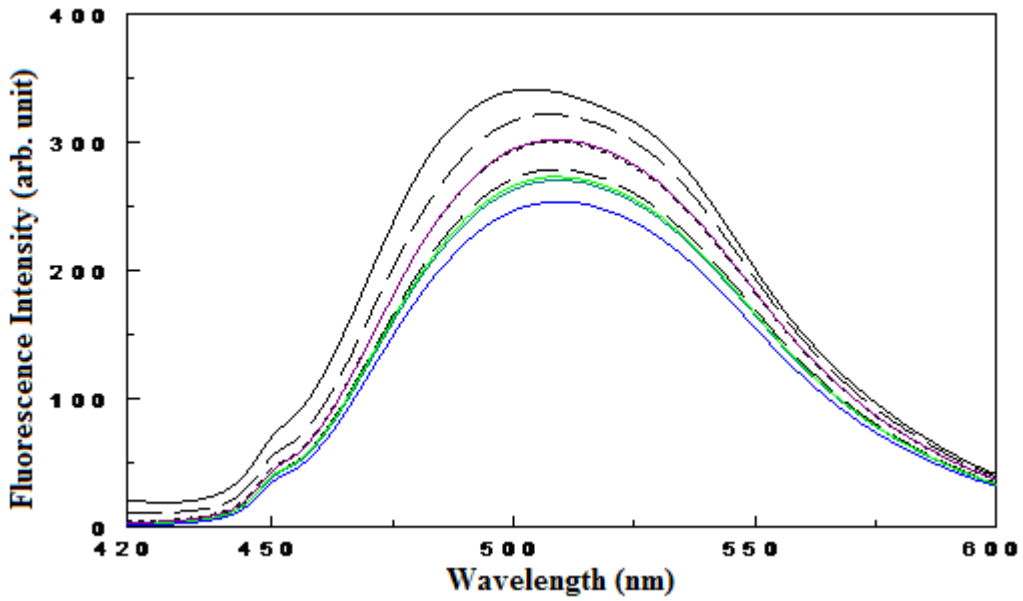

Figure 3.38: Fluorescence emission spectra of semi-cylindrical Cu-imp sensor containing BCM as a function of Cu^{2+} concentrations in DMSO. ($\lambda_{ex} = 410$ nm)

The fluorescence spectra of semi-cylindrical Cu(II)-ion imprinted sensor against Cu^{2+} titration in DMSO solution is shown in figure 3.38. Copper(II) ion titration experiment was carried out in DMSO since change in emission intensity of sensor was not observed in aqueous solution of Cu^{2+} ion.

As seen from figure 3.38. emission intensity of imprinted sensor is decreased upon interaction with BCM in DMSO. This shows that coordination interaction of Cu^{2+} ion in DMSO is favored by nitrogen atom in BCM.

On the other hand, nonimprinted material which was synthesized in the absence of copper(II) ion also exhibits similar Cu^{2+} ion induced emission spectra (figure 3.39). The plot of I/Io versus Cu^{2+} concentration shows that emission intensity of imprinted sensor is more quenched than that of nonimprinted material indicating the imprinting effect of sensor which was prepared in the presence of copper(II) ion.(Figure 3.40)

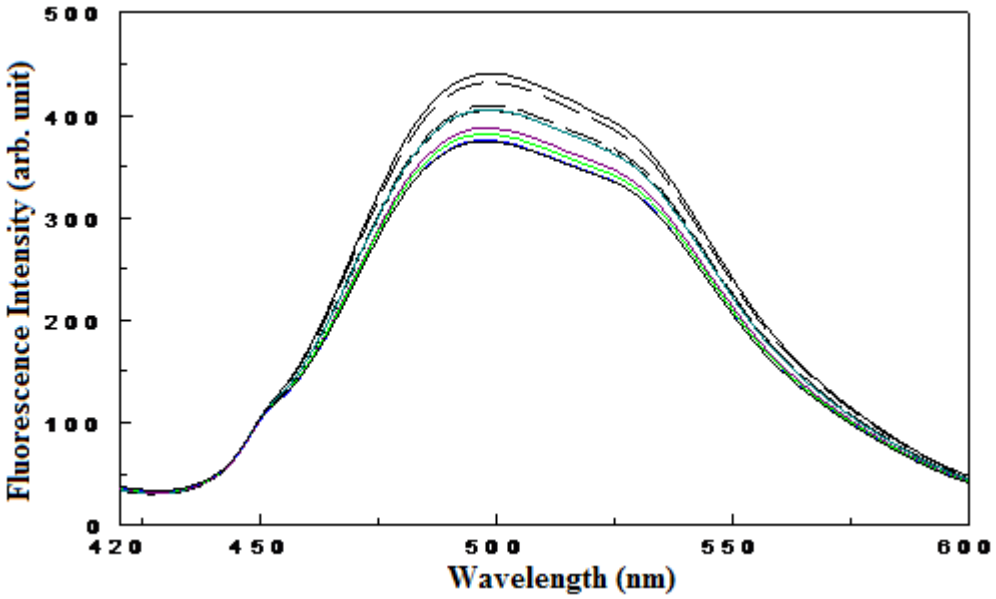

Figure 3.39: Emission spectra of semi-cylindrical nonimp polymer containing BCM depending on Cu^{2+} concentrations in DMSO. ($\lambda_{ex} = 410$ nm)

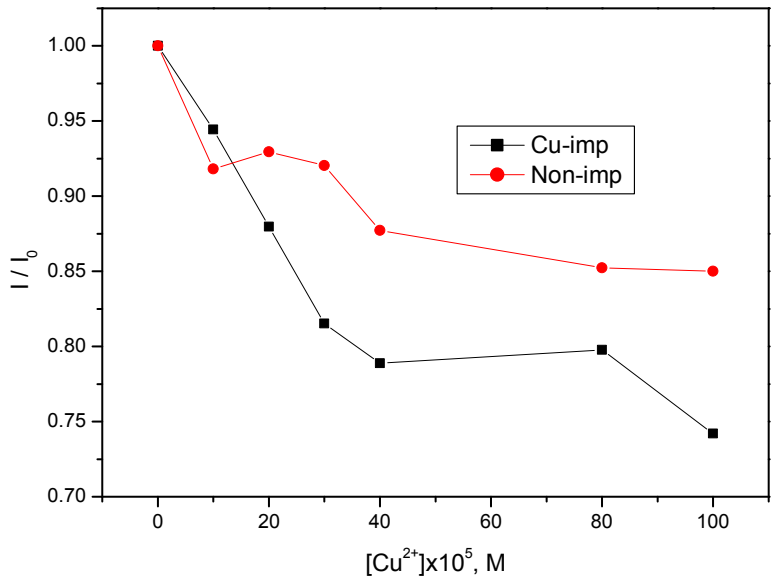

Figure 3.40: Cu^{2+} dependence of emission intensities of semi-cylindrical Cu-imp and nonimp polymers containing BCM in DMSO. ($\lambda_{ex} = 410$ nm)

4. CONCLUSION

The complex forming ability of VCz and BCM monomers with biologically important metal cations in organic solvents with different dipole moments and polarities were explored by carrying out fluorescence titration measurements. The results revealed that while the coordination of Zn^{2+} does not give visible changes of fluorescence emission, the coordination of paramagnetic transition-metal cations Pb^{2+}, Hg^{2+}, Fe^{2+} and Cu^{2+} partially or completely quenches the emission. On the other hand, interaction metal ions with fluorescent probes are more pronounced in solvents with low dipole moments.

FTIR-ATR spectroscopic measurements clarified that both of imprinted and nonimpirnted polymers have similar chemical structures after washing procedure, indicating the complete removal of metal ions from imprinted polymers. Imprinted polymers with VCz as a fluorescent molecule which were synthesized in the presence of the lead and iron ions combining two methacrylic acid monomers showed higher fluorescence quenching than those by the nonimprinted materials, where methacrylic acids were randomly distributed within the polymeric materials. Fluorescence measurements showed that the number of metal ions bound to VCz molecules in imprinted polymers were larger than those to the VCz in nonimprinted polymers. Thus, the larger quenching of the fluorescence intensities of the imprinted polymers can be accounted for by the increase of complexed metal ions with VCz. This provides evidence that a definite metal ion-binding site was formed, and the memory of pairing of methacrylic acids within the polymer was encoded, indicating the imprinting properties of the sensor materials. On the other hand, the results of the copper adsorption experiments show that the copper imprinted polymer containing VCz exhibits enhanced emission intensity upon addition of copper ion. Whereas quenching effect is observed when adding copper ion into the VCz monomer containing solution.

Spectrofluorometric investigation on photophysical and metal binding properties of newly synthesized BCM monomer revealed that mercury ion interaction is more pronounced in ethanol than 2-metoxyethanol and acetonitrile. On the other hand, fluorescent molecules sensing ability is increased when used low concentration of fluorescent probe in solution.

Fluorescence measurement applied to the polymers during the acid and base washing procedures showed that imprinted and nonimprinted polymeric materials exhibit pH dependence fluorescent emission. Fluorescence emissions of polymeric materials were more quenched at low and high pH values. Quenching efficiency of imprinted polymer depending on pH of the solution was higher than that of nonimprinted polymer. This result clarifies the formation of cavity in imprinted polymer allowing the hydronium or hydroxyl ions to reach the fluorescent molecules in side of the polymeric material.

Metal ion affinities of zinc and copper ions imprinted polymeric materials synthesized by template polymerization were monitirized by queching of emission intensity of BCM as a fluorescent probe used in both imprinted and non-imprinted materials. The results show that Hg^{2+} and Cu^{2+} metal ions cause to quenching of emission intensities of both imprinted and nonprinted polymers. But imp polymer displays higher quenching efficiency than that of nonimp material.

Finally, we have synthesized fluorescent polymeric materials which have VCz and BCM moieties as fluorescent chromophores and the MAA and Vim moieties imprinted as pairs in polymers to adsorb metal ions. We have found that chemosensor materials display sensitivity to the metal ions in a large range of concentrations and have potential of reuse. But the selectivity of polymeric materials in a mixture of metal ions solution needs to be developed.

References

[1]. **Kunieda T.,** 1982. Selective memory of synthetic macromolecules for their origins. J. Synth. Org. Chem. Jpn., **40**, 686–693.

[2]. **Bartels H, Prijs B.,** 1974. Specifically adsorbing silica gel.*Adv. Chromatogr.,* **11,** 115–143.

[3]. **C.A., Lorenzo, O.Güney, T. Tanaka et al.,** 2000, Polymer Gels That Memorize Elements of Molecular Conformation, *Macromolecules,* **33**,8693-8697.

[4]. **C.A., Lorenzo, O.Güney, T. Tanaka et al.,** 2000. Reversible Adsorption of Calcium ions by Imprinted Temperature Sensitive Gels, *J. Chem. Phys*., **114**(6), 2812-2816 .

[5]. **H. Hiratani, C. A, Lorenzo, J. Chuang. O. Güney, A.Y. Grosberg, T. Tanaka.,** 2001. Effect of Reversible Cross-Linker, N,N'-Bis(Acryloyl)-Cystamine, on Calcium ions Adsorption by Imprinted Gels, *Langmuir*., **17,**(14), 4431-4436 .

[6]. **O. Güney.,** 2003. Multiple-Point Adsorption of Terbium ions by Lead ion Templated Thermosensitive Gel: Elucidating Recognition of Conformation in Gel by Terbium Probe, *J. Mol. Recognit*; **16,** 67-71 .

[7]. **Tsukagoshi K, Murata M, Maeda M.,** 2001. In Molecularly Imprinted Polymers: Man-Made Mimics of Antibodies and their Applications in Analytical Chemistry, Techniques and Instrumentation in Analytical Chemistry, *Sellergren B (ed.). Elsevier: Amsterdam.*, **23,** 245–269.

[8]. **Tan TW, He XJ, Du WX.,** 2001. Adsorption behaviour of metal ions on imprinted chitosan resin. *J. Chem. Technol. Biotechnol*., **76,** 191–195.

[9]. **Molochnikov LS, Kovalyova EG, Zagorodni AA,Muhammed M, Sultanov YM, Efendiev AA.** 2003. Coordination of Cu(II) and Ni(II) in polymers imprinted so as to optimize amine chelate formation. *Polymer* ., **44,** 4805– 4815

[10] **Kabanov VA, Molochnikov LS, Il'ichev SA, Babkin ON, Sultanov YM, Grudzhev DD, Efendiev AA.,** 1986. An EPR study of copper(II) complexes with structured polymeric sorbents. *Polymer Science U. S. S. R.* **28,** 2736–2742.

[11]. **Ray A, Gupta SN.,** 1998. Construction of template polymeric ligand with 8-hydroxyquinoline. *J. Appl. Polym. Sci*., **67,** 1215–1219.

[12]. **Yamashita K, Nishimura T, Ohashi K, Ohkouchi H, Nango M.,** 2003. Two-step imprinting procedure of interpenetrating polymer network-type stimuli-responsive hydrogel-adsorbents. *Polym. J.,* **35:** 545–550.

[13]. **Wu JM, Wang YY, Yan CL.,** 2002. Selective adsorption of copper ion by copper ion templated alginate gel. *Chin. J.Anal. Chem*., **30,** 1414–1417.

[14]. **Kanekiyo Y, Inoue K, Ono Y, Shinkai S.,** 1998. Facile design of a metal-imprinted surface from a poly(vinyl chlorideco- acrylic acid) poly(propylene glycol) blend. *Tet. Lett*., **39,** 7721–7724

[15]. **Ray A, Gupta SN.,** 2001. Construction of metal template polymer with covalently bound dithizone. *J. Indian Chem.Soc*., **78,** 663–665.

[16]. **Zeng XF, Murray GM.,** 1996. Synthesis and characterization of site-selective ion-exchange resins templated for lead(II) ion. *Sep. Sci. Technol., **31,*** 2403–2418.

[17]. **Biju VM, Gladis JM, Rao TP.,** 2003. Ion imprinted polymer particles: synthesis, characterization and dysprosium ion uptake properties suitable for analytical applications.*Anal. Chim. Acta.,* **478,** 43–51.

[18]. **Biju VM, Gladis JM, Rao TP.,** 2003. Effect of irradiation of ion imprinted polymer (IIP) particles for the preconcentrative separation of dysprosium from other selected lanthanides. *Talanta.,* **60,** 747–754.

[19]. **Vigneau O, Pinel C, Lemaire M.,** 2002. Solid-liquid separation of lanthanide/lanthanide and lanthanide/actinide using ionic imprinted polymer based on a DTPA derivative. *Chem. Lett.,* **31:** 202–203.

[20]. **Singh A, Puranik D, Guo Y, Chang EI.,** 2000. Towards achieving selectivity in metal ion binding by fixing ligand-chelator complex geometry in polymers. *Reac. Func. Polym*., **44,** 79–89.

[21]. **Güney O, Yilmaz Y, Pekcan O.,** 2002. Metal ion templated chemosensor for metal ions based on fluorescence quenching. *Sens. Actuators B.,* **85,** 86–89.

[22]. **Murray GM, Jenkins AL, Bzhelyansky A, Uy OM.,** 1997.Molecularly imprinted polymers for the selective sequestering and sensing of ions. *Johns Hopkins APL Techn.Dig.,* **18,** 464–472.

[23]. **Say R, Birlik E, Ersöz A, Yilmaz F, Gedikbey T, Denizli A.,** 2003. Preconcentration of copper on ion-selective imprinted polymer microbeads. *Anal. Chim. Acta.,* **480,** 251–258.

[24]. **Daniel S, Gladis JM, Rao TP.,** 2003. Synthesis of imprinted polymer material with palladium ion nanopores and its analytical application. *Anal. Chim. Acta.,* **488,** 173–182.

[25]. **Sobhi DJ, Gladis JM, Rao TP.,** 2003. Synthesis of imprinted polymer material with palladium ion nanopores and its analytical application. *Anal. Chim. Acta.,* **488,** 173–182.

[26]. **Chen H, Olmstead MM, Albright RL, Devenyi J, Fish RH., 1**997. Metal-ion-templated polymers: synthesis and structure of N-(4- vinylbenzyl)-1,4,7-triazacyclononanezinc(II)complexes, their copolymerization with divinylbenzene,and metal-ion selectivity studies of the demetalated resins—Evidence for a sandwich complex in the polymer matrix. *Angew. Chem., Intl. Ed. Engl*., **36,** 642–645.

[27]. **Al-Kindy S, Badı´a R, Dı´az-Garcı´a ME.,** 2002. Fluorimetric monitoring of molecular imprinted polymer recognition events for aluminium. *Anal. Lett***., 35,** 1763–1774.

[28]. **Fujiwara I, Maeda M, Takagi M.,** 2003. Preparation of ferrocyanide-imprinted pyridine-carrying microspheres by surface imprinting polymerization. *Anal. Sci.,* **19,** 617–620.

[29]. **Cui A, Singh A, Kaplan DL.,** 2002. Enzyme-based molecular imprinting with metals. *Biomacromolecules.,* **3,** 1353–1358.

[30]. **Nakashima A, Isobe T.,** 1987. Metal ion-template syntheses of hybrid resins and the template effect on their selectivities for metal ions. *Memoirs of the Faculty of Science, Kyushu University, Series C.,* **16,** 33–42.

[31]. **Chanda M, Rempel GL.,** 1992. Enhanced copper selectivity and faster sorption kinetics of poly(4-vinylpyridine) crosslinked in presence of copper(II) as template on silica gel. Reac. Polym., **16,** 149–158.

[32]. **Kido H, Miyajima T, Tsukagoshi K, Maeda M, Takagi M.,** 1992. Metal-ion complexation behavior of resins prepared by a novel template polymerization technique. *Anal. Sci., **8,*** 749–753.

[33]. **Uezu K, Nakamura H, Goto M, Murata M, Maeda M,Takagi M, Nakashio F.,** 1994. Novel metal ion-imprinted resins prepared by surface template polymerization with W/O emulsion. *J. Chem. Eng. Jpn*., **27,** 436–438.

[34]. **Goto M.,** 2001. In Ion Exchange and Solvent Extraction, Ion Exchange and Solvent Extraction, *SenGupta AK, Marcus Y (eds). Marcel Dekker: New Yor.,;* **14,** 259–293.

[35]. **Su HJ, Wang ZX, Tan TW.,** 2003. Adsorption of Ni2ş on the surface of molecularly imprinted adsorbent from Penicillium chysogenum mycelium. *Biotechnol. Lett.,* **25,** 949–953.

[36]. **Makote RD, Dai S.,** 2001. Matrix-induced modification of imprinting effect for Cu^{2+} adsorption in hybrid silica matrices. *Anal. Chim. Act*a., **435,** 169–175.

[37] **Shustak G, Marx S, Turyan I, Mandler D.,** 2003. Application of sol-gel technology for electroanalytical sensing. *Electroanalysis.,* **15,** 398–408.

[38]. **Dhal PK.,** 2001. In Molecularly Imprinted Polymers: Man- Made Mimics of Antibodies and their Applications in Analytical Chemistry, Techniques and Instrumentation in Analytical Chemistry, *Sellergren B (ed.).Elsevier: Amsterdam.,* **23,** 185–201.

[39]. **Striegler S, Dittel M.,** 2003. Evaluation of new strategies to prepare templated polymers with sufficient oligosaccharide recognition capacity. *Anal. Chim. Acta.,* **484,** 53–62.

[40]. **Brunkan NM, Gagne´ MR.,** 2000. Effect of chiral cavities associated with molecularly imprinted platinum centers on the selectivity of ligand-exchange reactions at platinum. *J. Am. Chem. Soc.,* **122,** 6217–6225.

[41]. **Lin JM, Yamada M.,** 2001. Chemiluminescent flowthrough sensor for 1,10-phenanthroline based on the combination of molecular imprinting and chemiluminescence. *Analyst.,* **126,** 810–815.

[42]. **Tong AJ, Dong H, Li LD.,** 2002. Molecular imprintingbased fluorescent chemosensor for histamine using zinc (II)-protoporphyrin as a functional monomer. *Anal. Chim.Acta.,* **466,** 31–37.

[43]. **Hart BR, Shea KJ.,** 2002. Molecular imprinting for the recognition of N-terminal histidine peptides in aqueous solution. *Macromolecules.,* **35,** 6192–6201.

[44]. **Becker JJ, Gagne´ MR.,** 2003. Imprinting chiral information into rigidified dendrimers. *Organometallics.,* **22,** 4984–4998.

[45]. **Takeuchi T, Mukawa T, Matsui J, Higashi M, Shimizu KD.,** 2001. Molecularly imprinted polymers with metalloporphyrin-based molecular recognition sites coassembled with methacrylic acid. *Anal. Chem.,* **73,** 3869–3874.

[46]. **Sharma AC, Borovik AS.,** 2000. Design, synthesis, and characterization of templated metal sites in porous organic hosts: application to reversible dioxygen binding. *J. Am. Chem. Soc.,* **122,** 8946–8955.

[47]. **Sharma AC, Joshi V, Borovik AS.,** 2001. Surface grafting of cobalt complexes on polymeric supports: evidence for site isolation and applications to reversible dioxygen binding. *J. Polym. Sci. A,Polym. Chem.,* **39,** 888–897.

[48] **Sreenivasan K.,** 2001. The use of metal-containing monomer in the preparation of molecularly imprinted polymer to increase the adsorption capacity. *J. Appl. Polym. Sci.,* **80,** 2795–2799.

[49]. **Sreenivasan K, Sivakumar R.,** 2003. Ferric iron-containing molecularly imprinted polymer as an adsorbent for cholesterol. *Adsorption Science & Technology.,* **21,** 261–268.

[50]. **Wu LQ, Li YZ.,** 2003. Picolinamide-Cu(Ac)2-imprinted polymer with high potential for recognition of picolinamidecopper acetate complex. *Anal. Chim. Acta.,* **482,** 175–181.

[51]. **Matsui J, Nicholls IA, Takeuchi T, Mosbach K, Karube I.,** 1996. Metal ion mediated recognition in molecularly imprinted polymers. *Anal. Chim. Acta.,* **335,** 71–77.

[52]. **Jenkins AL, Uy OM, Murray GM.,** 1997. Polymer based lanthanide luminescent sensors for the detection of nevre agents. *Anal. Commun.,* **34,** 221–224.

[53]. **Mitchell-Koch JT, Borovik AS.,** 2003. Immobilization of a europium salen complex within porous organic hosts: modulation of luminescence properties in different chemical environments. *Chem. Mater.,* **15,** 3490–3495.

[54]. **Sellergren B, Shea KJ.,** 1993. Influence of polymer morphology on the ability of imprinted network polymers to resolve enantiomers. *J. Chromatogr.,* **635,** 31–49.

[55]. **Klein JU, Whitcombe MJ, Mulholland F, Vulfson EN.** 1999. Template-mediated synthesis of a polymeric receptor specific to amino acid sequences. *Angew. Chem. Intl. Ed. Engl.* **38,** 2057–2060.

[56] **Skudar K, Brüggemann O, Wittelsberger A, Ramström O.,** 1999. Selective recognition and separation of _-lactam antibiotics using molecularly imprinted polymers. *Anal.Commun.,* **36,** 327–331.

[57] **Sellergren B, Nilsson KGI.,** 1989. Molecular imprinting by multiple noncovalent host-guest interactions: synthetic polymers with induced specificity. *Methods Mol. Cell Biol*., **31,** 59–62.

[58]. **Sulitzky C, Ru¨ ckert B, Hall AJ, Lanza F, Unger K, Sellergren B.,** 2002. Grafting of molecularly imprinted polymer films on silica supports containing surface-bound free radical initiators. *Macromolecules.,* **35,** 79–91. .

[59]. **Pe´ rez N, Whitcombe MJ, Vulfson EN.,** 2000. Molecularly imprinted nanoparticles prepared by core-shell emulsion polymerization. *J. Appl. Polym. Sci.,* **77,** 1851–1859.

[60]. **Piletsky SA, Matuschewski H, Schedler U, Wilpert A,Piletska EV, Thiele TA, Ulbricht M.,** 2000. Surface functionalization of porous polypropylene membranes with molecularly imprinted polymers by photograft copolymerization in water. *Macromolecules.,* **33,** 3092–3098.

[61]. **Striegler S.,** 2002. Investigation of disaccharide recognition by molecularly imprinted polymers. *Bioseparation* **10,** 307–314

[62]. **Sreenivasan K.** 1998. Effect of the type of monomers of molecularly imprinted polymers on the interaction with steroids. *J. Appl. Polym. Sci.,* **68,** 1863–1866.

[63]. **Uezu K, Nakamura H, Kanno J, Sugo T, Goto M, Nakashio F.,** 1997. Metal ion-imprinted polymer prepared by the combination of surface template polymerization with postirradiation by _-rays. *Macromolecules.,* **30,** 3888–3891.

[64]. **Ru¨ ckert B, Hall AJ, Sellergren B.,** 2002. Molecularly imprinted composite materials via iniferter-modified supports.*J. Mater. Chem.,* **12,** 2275–2280.

[65] . **Li P, Rong F, Yuan CW.,** 2003. Morphologies and binding characteristics of molecularly imprinted polymers prepared by precipitation polymerization. *Polym. Int*., **52,** 1799–1806. .

[66] **Piletsky SA, Piletska EV, Karim K, Freebairn KW, Legge CH, Turner APF.,** 2002. Polymer cookery: influence of polymerization conditions on the performance of molecularly imprinted polymers. *Macromolecules.,* **35,** 7499– 7504.

[67]. **Kempe M.,** 1996. Antibody-mimicking polymers as chiral stationary phases in HPLC. *Anal. Chem.,* **68,** 1948–1953.

[68]. **Dong XC, Sun H, Lu XY, Wang HB, Liu SX, Wang N.,** 2002. Separation of ephedrine stereoisomers by molecularly imprinted polymers—influence of synthetic conditions and mobile phase compositions on the chromatographic performance. *Analystç.,* **127,** 1427–1432.

[69]. **Andersson L.,** 1988. Preparation of amino-acid esterselective cavities formed by non-covalent imprinting with a substrate in highly cross-linked polymers. *React. Polym. Ion Exch. Sorb*., **9,** 29–41.

[70]. **Shea KJ, Stoddard GJ, Shavelle DM, Wakui F, Choate RM.,** 1990. Synthesis and characterization of highly crosslinked polyacrylamides and polymethacrylamides—a new class of macroporous polyamides. *Macromolecules.,* **23,** 4497–4507.

[71]. **Zhan SZ, Dai Q, Yuan CW, Lu ZH, Haeussling L.,** 1999. Synthesis, recognition and separation of print molecule in molecularly imprinted polymers. *Anal. Lett.,* **32,** 677–687.

[72]. **Asanuma H, Kajiya K, Hishiya T, Komiyama M.,** 1999. Molecular imprinting of cyclodextrin in water for the recognition of peptides. *Chem. Lett.*,**28,** 665–666.

[73] **Ohkubo K, Sawakuma K, Sagawa T.,** 2001. Influence of cross-linking monomer and hydrophobic styrene comonomer on stereoselective esterase activities of polymer catalyst imprinted with a transition-state analogue for hydrolysis of amino acid esters. *Polymer.,* **42,** 2263–2266.

[74] **Shea KJ, Thompson EA.,** 1985. Site isolation in macroreticular divinylbenzene polymers. *Macromolecules.,* **18,** 814–817.

[75] **Yilmaz E, Mosbach K, Haupt K.,** 1999. Influence of functional and cross-linking monomers and the amount of template on the performance of

molecularly imprinted polymers in binding assays. *Anal. Commun.,* **36,** 167–170.

[76]. **Cooper AI, Hems WP, Holmes AB.,** 1999. Synthesis of highly cross-linked polymers in supercritical carbon dioxide by heterogeneous polymerization. *Macromolecules.,* **32,** 2156–2166.

[77] **Arshady R.,** 1992. Functional monomers. J. Macromo.Sci.—Rev. Macromol. *Chem. Phys. C., **32** ,* 101–132.

[78] **Karlsson JG, Andersson LI, Nicholls IA.,** 2001. Probing the molecular basis for ligand-selective recognition in molecularly imprinted polymers selective for the local anaesthetic bupivacaine. *Anal. Chim. Acta.,* **435,** 57–64.

[79] **Alexander C, Smith CR, Whitcombe MJ, Vulfson EN.,** 1999.Imprinted polymers as protecting groups for regioselectivemodification of polyfunctional substrates. *J. Am.Chem. Soc.,* **121,** 6640–6651.

[80]. **Ellwanger A, Berggren C, Bayoudh S, Crecenzi C,Karlsson L, Owens PK, Ensing K, Cormack P, Sherrington D, Sellergren B.,** 2001. Evaluation of methods aimed at complete removal of template from molecularly imprinted polymers. *Analyst.,* **126,** 784–792.

[81]. **Theodoridis G, Kantifes A, Manesiotis P, Raikos N,Tsoukali-Papadopoulou H.,** 2003. Preparation of a molecularly imprinted polymer for the solid-phase extraction of scopolamine with hyoscyamine as a dummy template molecule. *J. Chromatogr. A.,* **987,** 103–109.

[82]. **Martı´n-Esteban A, Turiel E, Stevenson D.,** 2001. Effect of template size on the selectivity of molecularly imprinted polymers for phenylurea herbicides. *Chromatographia .,* **53,** S434–S437.

[83]. **Zhang TL, Liu F, Chen W, Wang J, Li K.,** 2001. Influence of intramolecular hydrogen bond of templates on molecular recognition of molecularly imprinted polymers. *Anal. Chim. Acta.,* **450,** 53–61.

[84]. **Spivak DA, Campbell J.,** 2001. Systematic study of steric and spatial contributions to molecular recognition by non-covalent imprinted polymers. *Analyst.,* **126,** 793–797.

[85]. **Huang XD, Kong L, Li X, Zheng CJ, Zou HF.,** 2003. Molecular imprinting of nitrophenol and hydroxybenzoic acid isomers: effect of molecular structure and acidity on imprinting. *J. Mol. Recogn.,* **16,** 406–411.

[86]. **D'Oleo R, Alvarez-Lorenzo C, Sun G.,** 2001. A new approach to design imprinted polymer gels without using a template. *Macromolecules.,* **34,** 4965–4971.

[87]. **Andersson LI, Abdel-Rehim M, Nicklasson L, Schweitz L,Nilsson S.,** 2002. Towards molecular-imprint based SPE of local anaesthetics. *Chromatographia.,* **55,** S65–S69.

[88]. **Takeuchi T, Fukuma D, Matsui J.,** 1999. Combinatorial molecular imprinting: An approach to synthetic polymer receptors. Anal. Chem.,**71,** 285–290. DOI: 10.1021/ ac980858v

[89]. **Lanza F, Sellergren B.,** 1999. Method for synthesis and screening of large groups of molecularly imprinted polymers. *Anal. Chem.,* **71,** 2092–2096.

[90]. **Dirion B, Cobb Z, Schillinger E, Andersson LI, Sellergren B.,** 2003. Water-compatible molecularly imprinted polymers obtained via high-throughput synthesis and experimental design. *J. Am. Chem. Soc.,* **125,** 15101–15109.

[91]. **Takeuchi T, Fukuma D, Matsui J, Mukawa T.,** 2001. Combinatorial molecular imprinting for formation of atrazine decomposing polymers. *Chem. Lett.,* **30,** 530–531.

[92]. **D'Souza SM, Alexander C, Carr SW, Waller AM, Whitcombe MJ, Vulfson EN.,** 1999. Directed nucleation of calcite at a crystal-imprinted polymer surface. Nature., **398,** 312–316.

[93]. **Umpleby RJ, Rushton GT, Shah RN, Rampey AM, Bradshaw JC, Berch JK, Shimizu KD.,** 2001. Recognition directed site-selective chemical modification of molecularly imprinted polymers. *Macromolecules.,* **34,** 8446–8452.

[94]. **Kirsch N, Alexander C, Lu¨ bke M, Whitcombe MJ, Vulfson EN.,** 2000. Enhancement of selectivity of imprinted polymers via post-imprinting modification of recognition sites. *Polymer.,* **41,** 5583–5590.

[95]. **Koh JH, Larsen AO, White PS, Gagne´ MR.,** 2002. Disparate roles of chiral ligands and molecularly imprinted cavities in asymmetric catalysis and chiral poisoning. *Organometallics.,* **21,** 7–9.

[96]. **Ki CD, Oh C, Oh SG, Chang JY.,** 2002. The use of a thermally reversible bond for molecular imprinting of silica spheres. *J. Am. Chem. Soc*., **124,** 14838–14839.

[97] **Nicholls IA, Andersson HS.,** 2001. In Molecularly Imprinted Polymers: Man-Made Mimics of Antibodies and their Applications in Analytical Chemistry, Techniques and Instrumentation in Analytical Chemistry.*Sellergren B (ed.). Elsevier: Amsterdam*., **23**, 60–70.

[98] **Chianella I, Lotierzo M, Piletsky SA, Tothill IE, Chen BN, Karim K, Turner APF.,** 2002. Rational design of a polymer specific for microcystin-LR using a computational approach. *Anal. Chem.,* **74,** 1288–1293.

[99]. **Wu LQ, Sun BW, Li YZ, Chang WB.,** 2003. Study properties of molecular imprinting polymer using a computational approach. *Analyst.,* **128:** 944–949.

[100]. **Andersson HS, Nicholls IA.,** 1997. Spectroscopic evaluation of molecular imprinting polymerization systems.*Bioorg. Chem.,* **25,** 203–211.

[101]. **Svenson J, Andersson HS, Piletsky SA, Nicholls IA.,** 1998.Spectroscopic studies of the molecular imprinting selfassembly process. *J. Mol. Recogn*., **11,** 83–86.

[102]. **Katz A, Davis ME.,** 1999. Investigations into the mechanisms of molecular recognition with imprinted polymers. *Macromolecules.,* **32,** 4113–4121. DOI: 10.1021/ma981445z

[103]. **Lanza F, RutherM, Hall AJ, Dauwe C, Sellergren B.,** 2002 In Molecularly Imprinted Materials-Sensors And Other Devices,MRS Symposium Proceedings, Vol. 723, Shea KJ,Yan M, Roberts MJ, Cremer PS, Crooks RM, Sailor MJ (eds). Materials Research Society: Warrendale, Pennsylvania., 93–103.

[104]. **Kim H, Spivak DA.,** 2003. New insight into modeling noncovalently imprinted polymers. J. Am. Chem. Soc., **125**,11269–11275

[105]. **O'Brien TP, Grinberg N, Bicker G, Wyvratt J, Snow NH.,** 2002. Evaluation of the origins of the selectivity of polymers imprinted with a HIV protease inhibitor using infrared spectroscopy and high performance liquid chromatography. *Enantiomer*., **7,** 139–148.

[106]. **Srebnik S, Lev O.,** 2002. Toward establishing criteria for polymer imprinting using mean-field theory.J. Chem. Phys., **116,** 10967–10972.

[107]. **Pande VS, Grosberg AY, Tanaka T.,** 1994. Thermodynamic procedure to synthesize heteropolymers that can renature to recognize a given target molecule. *Proc. Natl.Acad. Sci. USA*., **91,** 12976–12979.

[108] **Pande VS, Grosberg AY, Tanaka T.,** 1994. Folding thermodynamics and kinetics of imprinted renaturable heteropolymers.*J. Chem. Phys.,* **101,** 8246–8257.

[109]. **Pande VS, Grosberg AY, Tanaka T.,** 1997. How to create polymers with protein-like capabilities: a theoretical suggestion.*Physica D.,* **107,** 316-321.

[110]. **Tanaka T, Enoki T, Grosberg AY, Masamune S, Oya T,Takaoka Y, Tanaka K, Wang CN, Wang GQ.,** 1998. Reversible molecular adsorption as a tool to observe freezing and to perform design of heteropolymer gels. *Berichte Der Bunsen-Gesellschaft-Physical Chemistry Chemical Physics.,* **102,** 1529–1533.

[111]. **Enoki T, Tanaka K, Watanabe T, Oya T, Sakiyama T, Takeoka Y, Ito K, Wang GQ, Annaka M, Hara K, Du R,Chuang J, Wasserman K, Grosberg AY, Masamune S,Tanaka T.,** 2000. Frustrations in polymer conformation in gels and their minimization through molecular imprinting.*Phys. Rev.* Lett., **85,** 5000–5003.

[112]. **Ito K, Chuang J, Alvarez-Lorenzo C, Watanabe T, Ando N,Grosberg AY.,** 2003. Multiple point adsorption in a heteropolymer gel and the Tanaka approach to imprinting:experiment and theory. *Prog. Polym. Sci.,* **28,** 1489–1515.

[113]. **Rzysko W, Sokolowski S, Pizio O.,** 2002. Theory of adsorption in a polydisperse templated porous material: hard sphere systems. *J. Chem. Phys.,* **116,** 4286–4292.

[114] **Shea KJ, Spivak DA, Sellergren B.,** 1993. Polymer complements to nucleotide bases—selective binding of adenine derivatives to imprinted polymers. *J. Am. Chem. Soc*., **115,** 3368–3369.

[115] **Cheong SH, Rachkov AE, Park JK, Yano K, Karube I.,** 1998.Synthesis and binding properties of a noncovalent molecularly mprinted testosterone-specific polymer. *J.Polym. Sci. A,Polym. Chem.,* **36,** 1725–1732.

[116] **Umpleby RJ, Baxter SC, Bode M, Berch JK, Shah RN,Shimizu KD.,** 2001. Application of the Freundlich adsorption isotherm in the characterization of molecularly imprintedpolymers. *Anal. Chim. Acta.,* **435,** 35–42.

[117] **Yang G, Wang D, Li Z, Zhou S, Chen Y.,** 2003. Adsorption isotherms on aminoantipyrine imprinted polymer stationary phase. *Chromatographia.,* **58,** 53–58.

[118]. **Umpleby RJ, Baxter SC, Chen YZ, Shah RN, Shimizu KD.,** 2001. Characterization of molecularly imprinted polymers with the Langmuir-Freundlich isotherm. *Anal. Chem.,* **73:**4584–4591

[119]. **Turiel E, Perez-Conde C, Martin-Esteban A.,** 2003. Assessment of the cross-reactivity and binding sites characterisation of a propazine-imprinted polymer using the Langmuir-Freundlich isotherm. *Analyst.,* **128,** 137–141.

[120]. **Umpleby RJ, Bode M, Shimizu KD.,** 2000. Measurement of the continuous distribution of binding sites in molecularly imprinted polymers. *Analyst.,* **125,** 1261–1265.

[121] **Chen WY, Chen CS, Lin FY.,** 2001. Molecular recognition in imprinted polymers: thermodynamic investigation of analyte binding using microcalorimetry. *J. Chromatogr.A.,* **923,** 1-6.

[122] **Weber A, Dettling M, Brunner H, Tovar GEM.,** 2002. Isothermal titration calorimetry of molecularly imprinted polymer nanospheres. Macromol. *Rapid Commun.,* **23,**824–828.

[123]. **Wandelt B, Mielniczak A, Turkewitsch P, Wysocki S.,** 2003.Steady-state and time-resolved fluorescence studies of fluorescent imprinted polymers. *J. Lumin.,* **102-103,** 774–781.

[124]. **Kostrewa S, Emgenbroich M, Klockow D, Wulff G.,** 2003.Surface-enhanced Raman scattering on molecularly imprinted polymers in water. Macromol. *Chem. Phys.,* **204,** 481–487.

[125]. **Al-Kindy S, Badı´a R, Sua´ rez-Rodrı´guez JL, Dı´az-Garcı´a ME.,** 2000. Molecularly imprinted polymers and optical sensing applications. *Crit. Rev. Anal. Chem.,* **30,**291–309.

[126]. **Piletsky SA, Piletskaya K, Piletskaya EV, Yano K, Kugimiya A, Elgersma AV, Levi R, Kahlow U, Takeuchi T, Karube I, Panasyuk TI, El'Skaya AV.,** 1996. A biomimetic receptor system for sialic acid based on molecular imprinting.*Anal. Lett.,* **29,** 157–160.

[127] **Piletsky SA, Terpetschnig E, Andersson HS, Nicholls IA,Wolfbeis OS.,** 1999. Application of non-specific fluorescent dyes for monitoring

enantio-selective ligand binding to molecularly imprinted polymers. *Fresenius' J. Anal Chem.,* **364,** 512–516.

[128] **Rathbone DL, Su DQ, Wang YF, Billington DC.,** 2000.Molecular recognition by fluorescent imprinted polymers.*Tet. Lett.,* **41,** 123–126.

[129] **Thanh NTK, Rathbone DL, Billington DC, Hartell NA.,** 2002.Selective recognition of cyclic GMP using a fluorescencebased molecularly imprinted polymer. *Anal. Lett.,* **35,**2499–2509.

[130] **Gao SH, Wang W, Wang BH.,** 2001. Building fluorescent sensors for carbohydrates using template-directed polymerizations.*Bioorg. Chem.*,**29,** 308–320.

[131]**. Lulka MF, Iqbal SS, Chambers JP, Valdes ER, Thompson RG, Goode MT, Valdes JJ.,** 2000. Molecular imprinting of Ricin and its A and B chains to organic silanes: fluorescence detection. *Mater. Sci. Eng.,* **11,** 101–105.

[132] **Kriz D, Ramstro¨m O, Svensson A, Mosbach K.,** 1995.Introducing biomimetic sensors based on molecularlyimprinted polymers as recognition elements. *Anal.Chem.,* **67,** 2142–2144.

[133] **Kriz D, Ramstro¨mO, Mosbach K.,** 1997. Molecular imprinting—New possibilities for sensor technology. *Anal. Chem.,* **69**, A345–A349.

[134] **Turkewitsch P, Wandelt B, Darling GD, Powell WS.** 1998.Fluorescent functional recognition sites through molecular imprinting. A polymer-based fluorescent chemosensor for aqueous cAMP. *Anal. Chem*. **70,** 2025–2030.

[135] **Wandelt B, Turkewitsch P, Wysocki S, Darling GD.,** 2002.Fluorescent molecularly imprinted polymer studied by time-resolved fluorescence spectroscopy. *Polymer.,* **43,**2777–2785.

[136] **Sua´ rez-Rodrı´guez JL, Dı´az-Garcı´a ME.,** 2000. Flavonol fluorescent flow-through sensing based on a molecular imprinted polymer. *Anal. Chim. Acta.,* **405,** 67–76.

[137]. **Sua´ rez-Rodrı´guez JL, Carvalho-Torres AL, Paredes-Nachon I, Badı´a R, Marcos-Pascual C, Dı´az-Garcı´a ME.,** 1999. Molecularly imprinted polymers for developing biomimetic optical sensors. *Quimica Analitica.,* **18,** 20–22.

[138]**Lulka MF, Chambers JP, Valdes ER, Thompson RG,Valdes JJ.,** 1997. Molecular imprinting of small molecules with organic silanes: fluorescence detection. *Anal. Lett*., **30,** 2301–2313.

[139]**Nopper D, Lammershop O, Wulff G, Gauglitz G.,** 2003. Amidine-based molecularly imprinted polymers—new sensitive elements for chiral chemosensors. *Anal. Bioanal.Chem.,* **377,** 68–613.

BIOGRAPHY

Salih SUBAŞI was born in Ardahan in 1978. He graduated from Yalova High School - Yalova in 1995. He started his undergraduate education in Marmara University, Chemistry Department, and obtained BSc degree at Chemistry Department in January, 2000. After his graduation, he attended in Istanbul Technical University, Polymer Science and Technology, where he has prepared hereby master thesis.